Current Research (2026) Newfoundland and Labrador Department of Energy and Mines Geological Survey, Report 26-1, pages 205-226

PETROGRAPHY AND MINERAL CHEMISTRY OF Li-BARREN PEGMATITES IN NEWFOUNDLAND, AS AN INDICATOR OF CRITICAL MINERAL (Li, Cs AND Ta) PROSPECTIVITY

J. Conliffe, K.M. Malay[1,2] and D.B. Archibald[1]
Mineral Deposits Section
[1]Earth and Environmental Sciences Department, St. Francis Xavier University, Antigonish, NS, B2G 2W5
[2]Department of Earth Sciences, Memorial University of Newfoundland, St. John's, NL, A1B 3X5

ABSTRACT

*Li-enriched pegmatites, containing Li minerals such as spodumene, lepidolite or petalite, are an important global source of Li, Cs and Ta as well as a number of other critical minerals, but exploration for them is difficult due to the relatively small spatial footprint of pegmatites. However, Li-barren pegmatites (*i.e.*, pegmatites with no Li-minerals) are much more widespread, and the petrography and mineral chemistry of these pegmatites are important in understanding magmatic fractionation and the possible association between Li-barren and Li-enriched pegmatites.*

*This study presents the results of detailed petrographic and mineral chemistry (*in-situ *EPMA and LA-ICP-MS) analyses from three areas of known pegmatites in Newfoundland. Li-barren pegmatites in the Peter Snout area are spatially associated with Li-enriched pegmatites (Killick pegmatite field and Hydra pegmatite), whereas Li-barren pegmatites in Snowshoe Pond and the Cape Freels areas have no known association with Li-enriched pegmatites. Detailed mineralogical studies show that the main minerals present in Li-barren pegmatites in all areas are similar, but pegmatites from the Peter Snout area are characterized by the presence of abundant accessory columbite-group minerals, which are rare or absent in in Snowshoe Pond and the Cape Freels areas. Mineral chemistry data from feldspars, micas, garnet, tourmaline and beryl also show significant variations between the three study areas, which point to increased magmatic fractionation in the Peter Snout area compared to the other two studied areas. In particular, low K/Rb, and elevated Cs and Ga values in muscovite, low K/Rb and elevated Rb, Cs, Li and Ga in K-feldspar, and the presence of Mn-enriched garnets with elevated Nb and Ta contents in Li-barren pegmatites from the Peter Snout area are consistent with a higher degree of magmatic fractionation and increased magmatic fertility. These criteria can be used to assess magmatic fractionation and mineral potential from other Li-barren pegmatites elsewhere in Newfoundland and Labrador.*

INTRODUCTION

Lithium–cesium–tantalum (LCT) pegmatites are an important global source of lithium, accounting for most of the world's global lithium supply (USGS, 2025); and include numerous other critical minerals such as cesium, tantalum, beryllium, high-quality silica and feldspar (Linnen *et al.*, 2012; Bradley *et al.*, 2017; McCaffrey and Jowitt, 2023). Despite their economic importance, the origin of LCT pegmatites is not fully understood, with debate ongoing on the source of Li-enriched melt and role of magmatic vs. anatectic melting during formation of these intrusions (Černý, 1991; London, 2008, Müller *et al.*, 2017; Knoll *et al.*, 2023, Koopmans *et al.*, 2024). In addition, there is commonly overlapping spatial distribution of Li-enriched pegmatites (containing Li minerals such as spodumene, lepidolite or petalite) and Li-barren pegmatites (with no Li minerals) in the same area (Roda-Robles *et al.*, 2023; Curry *et al.*, 2025). The complex distribution of Li-minerals in these pegmatites also results in pegmatite dykes that may be Li-enriched in some areas and Li-barren in others (Dias *et al.*, 2025). This has important implications for mineral exploration, as it is imperative to determine if the much more abundant Li-barren pegmatites represent less fractionated variant of Li-enriched pegmatites, or are simply unfractionated granitic melts that are unlikely to be related to economically significant mineralization. Recent studies have shown that mineral chemistry is an effective tool in determining the prospectivity of Li-barren pegmatites (Maneta and Baker, 2019; Wise *et al.*, 2024; Curry *et al.*, 2025; Dias *et al.*, 2025; Tvauri *et al.*, 2025), with certain minerals (*e.g.*, mica, K-feldspar, tourmaline) particularly effective indicators of melt

evolution due to the incorporation of various trace elements (*e.g.*, Li, Rb, Cs, Zn, Nb, Ta) during fractional crystallization. The variable enrichment of these elements can be compared with Li-enriched pegmatites, which provides insights into the relationship between pegmatite bodies and guide future exploration efforts, particularly using handheld geochemical analyzers such as portable X-ray fluorescence (XRF) and laser-induced breakdown spectroscopy (LIBS) equipment.

This report presents the results of mineralogical and mineral chemistry studies on pegmatites from three areas in central and southern Newfoundland (Figure 1). These include the Peter Snout area, where Li-barren pegmatites are spatially associated with known Li-enriched pegmatites (Killick and Hydra pegmatite fields; Conliffe *et al.*, 2024), as well as the Snowshoe Pond and Cape Freels areas. This report includes a combination of field observations, petrography and mineral trace-element geochemistry to characterize the pegmatites from each study area. The results are compared to published data from Li-enriched and Li-barren pegmatites in other global settings to assess the relative prospectivity of these areas. Ongoing work includes comparisons with mineralogy and mineral chemistry of Li-

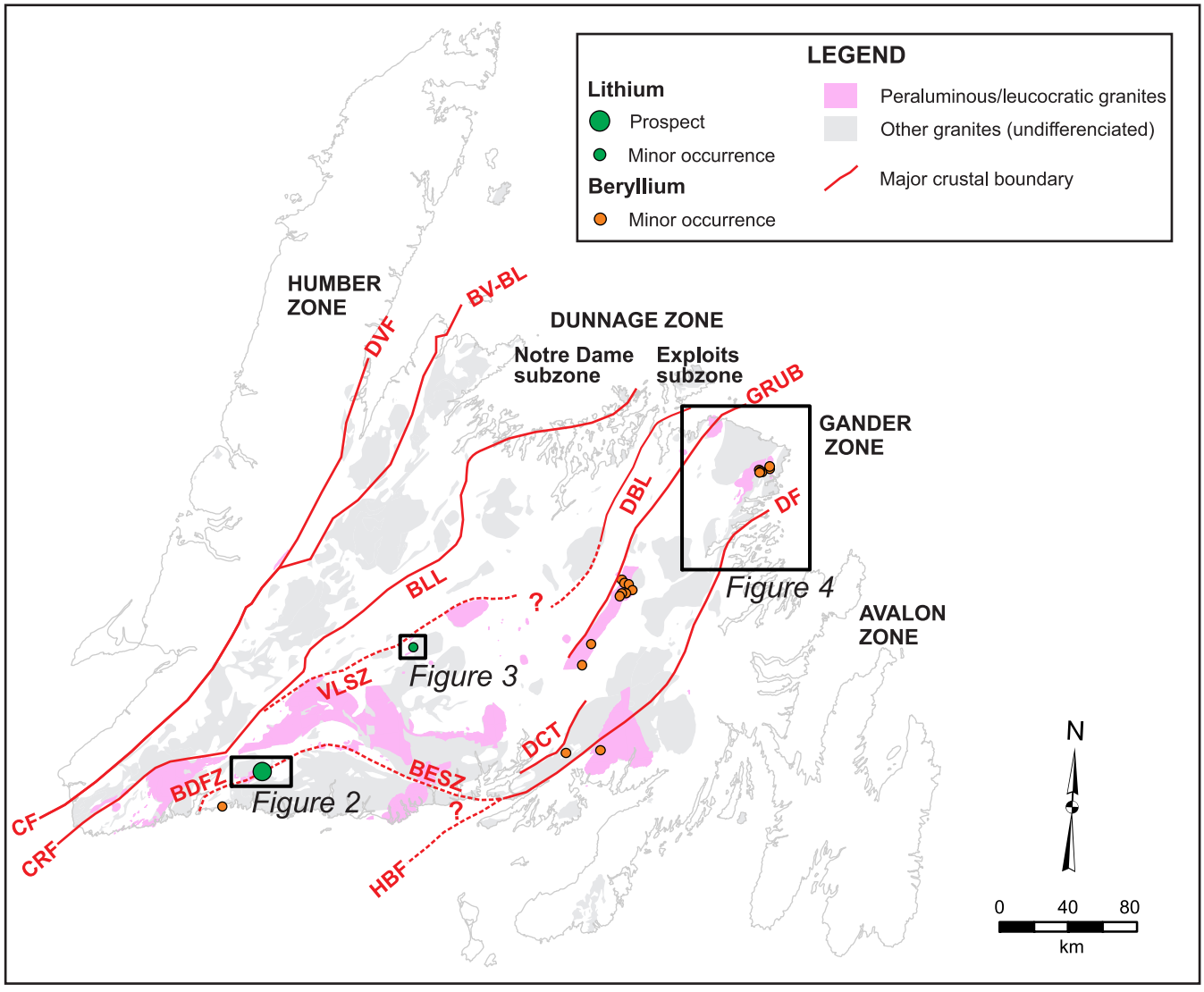

Figure 1. *Simplified geological map of the island of Newfoundland, showing major lithotectonic zones, large-scale crustal structures, distribution of Silurian to Devonian peraluminous and leucocratic granites, and location of lithium and beryllium occurrences associated with granites (adapted from ColmanSadd* et al.*, 1990). BDFZ–Bay d'Est Fault Zone, BESZ–Bay d'Espoir Shear Zone, BLL-Beothuk Lake Line, BV-BL–Baie Verte-Brompton Line, CF–Cabot Fault, CRF–Cape Ray Fault, DBL–Dog Bay Line, DCT–Day Cove Thrust, DF–Dover Fault, DVF–Doucers Valley Fault Zone, GRUB–Gander River Ultrabasic Belt, HBF–Hermitage Bay Fault, VLSZ–Victoria Lake Shear Zone. Location of Figures 2 to 4 shown.*

enriched pegmatites in southern Newfoundland to understand the geochemical evolution of pegmatites in Newfoundland, as well as comparing the detailed mineral chemistry data obtained during this study with data from handheld pXRF and LIBS studies to assess the effectiveness of these techniques during regional mineral exploration.

REGIONAL GEOLOGY

Ganderia is a complex peri-Gondwanan composite terrane in the northern Appalachians, which was accreted to composite Laurentia during the Paleozoic (Hibbard *et al.*, 2007; Pollock *et al.*, 2012; van Staal *et al.*, 2012, 2021). Ganderia is derived from the Amazonian margin of Gondwana and drifted across the Iapetus Ocean until its final collision with Laurentia during the Silurian Salinic Orogeny (van Staal *et al.*, 1996, 2021; Lin *et al.*, 2007; Schulz *et al.*, 2008). Ganderia is composed of a series of leading arc backarcs (Penobscot and Victoria-Exploits arcs) and a trailing margin comprised of continent-derived passive margin sediments known as the Gander Margin (van Staal and Barr, 2012; van Staal *et al.*, 2021). The Gander Margin corresponds to the Gander Zone of Williams (1979) and consists predominantly of Cambrian to Silurian metasedimentary rocks which were deposited on Neoproterozoic basement (van Staal and Barr, 2012; van Staal *et al.*, 2021). The Gander Margin metasedimentary rocks are locally overlain by Late Silurian to Early Devonian volcano-sedimentary rocks, including the La Poile Group in southern Newfoundland (O'Brien *et al.*, 1991). At least three phases of syn- to posttectonic Silurian and Devonian granitic magmatism affected the Gander Margin, which are associated with the Acadian orogenic cycle (Wang *et al.*, 2024). Wang *et al.* (2024) attributed these magmatic cycles to subduction (435–420 Ma), syncollisional (415–405 Ma) and postcollision (395–370 Ma) settings in the Acadian orogenic cycle and identified regional-scale migration of magmatism over time.

PEGMATITES IN THE GANDER MARGIN

Numerous swarms of pegmatite dykes that intrude metasedimentary rocks of the Gander Margin have been reported during regional mapping (*e.g.*, Jayasinghe, 1978; Chorlton, 1980a, b; O'Brien, 1982; Colman-Sadd, 1987a; O'Neill, 1991, 1992). The first attempt at a detailed study of pegmatite occurrences in Newfoundland was by Tater (1964), who conducted field studies in areas of known pegmatite occurrences and discussed their geological characteristics and economic possibilities. This was followed up in 1965 and 1966 by more detailed mapping and sampling of pegmatites in locations identified during the earlier work and investigation of other areas for similar pegmatite occurrences (Gale, 1966, 1967). Much of this focused on the Cape Freels area, where multiple beryl-bearing pegmatites were identified associated with muscovite–biotite-bearing peraluminous granites. Other areas studied included coastal sections in southwestern Newfoundland from Port aux Basque to Grey River, as well as areas in central and northern Newfoundland (Tater, 1964; Gale, 1966, 1967). Following these initial assessments in the 1960s, studies of pegmatites in Newfoundland were restricted to field observations made during regional bedrock mapping programs.

The presence of rare-element-enriched pegmatites in central Newfoundland was first reported from the Snowshoe Pond area by Magyarosi (2020) during regional studies following up anomalously high fluorine concentrations in till. Based on their geochemical and mineralogical characteristics, Magyarosi (2020) classified these pegmatites as LCT-type pegmatites, and they represented the first reported lithium occurrence in Newfoundland and Labrador. This was followed in 2021 by the discovery of LCT pegmatites in the Peter Snout area, ~30 km north of Burgeo by Benton Resources Inc. and Sokoman Minerals Corp. Exploration in this area since 2021 has identified spodumene and pollucite-bearing LCT pegmatites over a 10 km strike length, which is collectively known as the Killick Lithium Project (Conliffe *et al.*, 2024). Following this discovery, a collaborative research project was initiated between St. Francis Xavier University, Vinland Lithium Inc., Memorial University of Newfoundland, the Geological Survey of Canada and the GSNL to investigate the geological controls on formation of LCT pegmatites in southwestern Newfoundland and mineral potential for other granite-related critical minerals (Li, Cs, W, Mo, Sn, Ta, Bi).

METHODOLOGY

Fieldwork in the three study areas was conducted between 2022 and 2025 and included collection of detailed field observations of pegmatites and associated host rocks, and collection of rock samples for petrographic and lithogeochemical studies. A total of 18 Li-barren pegmatite samples were collected for this study (Table 1), ten from the Burgeo area, five from the Cape Freels area and three from the Snowshoe Pond area (including one sample previously collected by Z. Magyarosi). Thin sections were prepared from each sample for petrographic analysis, and five samples were analyzed using a FEI MLA 650FEG scanning electron microscope (SEM-MLA) at the Memorial University of Newfoundland Micro Analysis Facility (MUN MAFIIC). Following detailed petrographic analysis, suitable grains of plagioclase, K-feldspar, muscovite, garnet, tourmaline, beryl and biotite were selected for mineral chemistry analysis.

Table 1. Location of Li-barren pegmatites analyzed in this study, including mineralogy and host lithologies

Sample	Project	Mineralogy	Host rocks	Latitude	Longitude	SEM	EPMA	LA
22JC117B01	Burgeo	qz-ms-mc-ab-gnt	Dolman Cove Formation	47.832	-58.037	x	x	x
22JC123B01	Burgeo	ab-qz-mc-ms-gnt	Rose Blanche Granite	47.850	-57.853	x	x	
23JC013A01	Burgeo	qz-ab-ms-tur-mc-gnt	Dolman Cove Formation	47.847	-57.818	x	x	x
23JC026A01	Burgeo	qz-ms-ac-mc-gnt	Dolman Cove Formation	47.915	-57.719		x	x
23JC061A01	Burgeo	qz-mc-ms-ab-brl-gnt-mol	Dolman Cove Formation	47.861	-57.753			x
24JC033A01	Burgeo	ab-qz-ms-mc-gnt	Dolman Cove Formation	47.888	-57.702	x	x	x
24JC039A01	Burgeo	ab-qz-ms-mc-brl-gnt	Dolman Cove Formation	47.875	-57.737	x	x	x
25JC008B01	Burgeo	qz-ab-ms-mc-brl-gnt	Peter Snout Granite	47.852	-57.821		x	x
25JC011B01	Burgeo	qz-ms-mc-ab	Dolman Cove Formation	47.862	-57.748		x	x
25JC011B02	Burgeo	ab-qz-gnt-ms	Dolman Cove Formation	47.862	-57.748		x	x
23JC095B01	Cape Freels	qz-ms-mc-ab-gnt	Hare Bay Gneiss	49.156	-53.633		x	x
23JC113C01	Cape Freels	mc-qz-ms-ab-gnt	Wareham Granite	49.061	-53.848		x	x
24JC106A01	Cape Freels	qz-ab-mc-tur-ms-gnt	Business Cove Granite	49.178	-53.640		x	x
24JC152A01	Cape Freels	qz-ms-mc-ab-gnt	Gander Group	49.161	-54.167		x	x
24JC160B01	Cape Freels	ab-qz-ms-mc-tur-gnt	Gander Group	48.698	-54.223	x	x	x
18ML064A03	Snowshoe	qz-mc-ab-ms-gnt	Spruce Brook Formation	48.434	-56.577			x
24JC028A01	Snowshoe	ms-qz-mc-ab-bt	Spruce Brook Formation	48.402	-56.640		x	x
24JC029A01	Snowshoe	qz-ab-ms-mc-gnt	Spruce Brook Formation	48.402	-56.639		x	x

ELECTRON PROBE MICRO-ANALYSIS (EPMA)

The EPMA data were collected using a JEOL JXA-8230 microprobe at the Electron Probe Microanalytical facility at Memorial University. For most silicates, FeO, MnO, TiO_2, K_2O, CaO, Na_2O, Al_2O_3, SiO_2, MgO, Nb_2O_5, NiO, P_2O_6, Ta_2O_5, Cr_2O_3, Cl and F were measured, B_2O_3 was also measured in tourmaline and BeO was calculated for beryl. The detection levels for major and minor elements are around 0.01 wt. %. For garnet, a spot measurement was used with a 15 aV, and almandine garnet was the reference material. Beryl was measured with a 3 micron diameter spot at 15 aV, with a spodumene standard. All other minerals were measured with a 5 micron diameter spot at 15 aV, with an albite standard for feldspar, biotite standard for mica and a tourmaline standard for tourmaline. Background measurements were run for half of the peak analysis time on each side, and after every twenty to twenty-five unknowns measured, three reference materials were analyzed to ensure accuracy of measurement. Structural formula calculations were performed using custom spreadsheets and calculated atoms per formula units (apfu) and are included in the supplementary data tables.

LASER ABLATION-INDUCTIVELY COUPLED PLASMA-MASS SPECTROMETRY (LA-ICP-MS)

In situ LA-ICP-MS analyses were performed at the Micro Analysis Facility within the Core Research and Instrument Training Network (CREAIT) at Memorial University using a GeoLas 193 nm ArF excimer Laser (Coherent, CompexPro) connected to Thermo Scientific Element XR sector field ICP MS. The laser was operated at constant HV, with a repetition rate of 10 Hz in spot scan mode (400 pulses). Ablation employed a spot diameter of 40 µm during ablation wherein a fluence of 4 J/cm^2 is maintained. Sample introduction was achieved by a ~1 L/min He flow with Ar (sample gas, ~0.85 L/min) mixed into the sample introduction tubing right before the interface. The Element XR interfaces was fitted with standard Ni sample and H skimmer cones, mass acquisition was performed in low resolution mode. Acquired masses include ^{6}Li, ^{9}Be, ^{11}B, ^{27}Al, ^{43}Ca, ^{45}Sc, ^{49}Ti, ^{53}Cr, ^{55}Mn, ^{57}Fe, ^{59}Co, ^{66}Zn, ^{71}Ga, ^{85}Rb, ^{88}Sr, ^{89}Y, ^{90}Zr, ^{93}Nb, ^{111}Cd ^{115}In, ^{118}Sn, ^{133}Cs, ^{137}Ba, ^{139}La, ^{140}Ce, ^{141}Pr, ^{146}Nd, ^{147}Sm, ^{153}Eu, ^{157}Gd, ^{159}Tb, ^{163}Dy, ^{165}Ho, ^{166}Er, ^{169}Tm, ^{172}Yb, ^{175}Lu, ^{178}Hf, ^{181}Ta, ^{182}W, ^{208}Pb, ^{232}Th and ^{238}U (100 samples per peak, 5% mass window and 0.002 s acquisition time). For each spot / profile, a gas blank was analyzed for 30 s, followed by 40 s of ablation. Primary reference materials were NIST glasses 610 and 612 (Pearce *et al.*, 1997, Jochum *et al.*, 2011). Data reduction was performed offline *via* the trace element data reduction algorithm of the Iolite 3 program suite (Paton *et al.*, 2011), with Si as an internal standard channel.

PEGMATITES IN THE PETER SNOUT AREA

The presence of pegmatites in the Peter Snout area (NTS 11P/13) was first noted by Chorlton (1980a, b), who reported on abundant pegmatites and tourmaline-bearing dykes concentrated around the Bay d'Est Fault (Figure 2). These include the Li-enriched Killick Pegmatite field, with multiple spodumene bearing dykes exposed over an area of ~1 x 2 km,

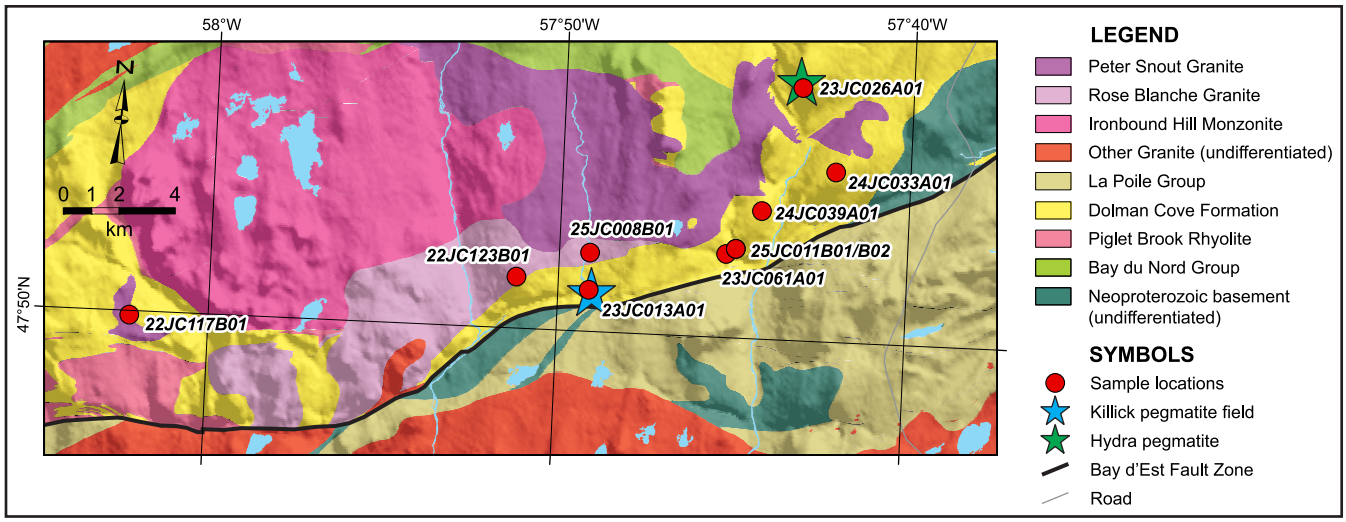

Figure 2. *Geological map of the Peter Snout area, showing major geological units, sample locations, Killick pegmatite field and Hydra Pegmatites. Adapted from Chorlton (1980a, b) and O'Brien (1982).*

and Hydra pegmatite, a 2–8-m thick-zoned pegmatite grading up to 8.75% Cs_2O and 0.41% Li_2O over a 1.2 m channel sample (Conliffe *et al.*, 2024). The geological setting of these pegmatites has been described in detail by Conliffe *et al.* (2024), Saha *et al.* (2025) and Malay *et al.* (2025).

In addition to these known mineralized pegmatites, numerous Li-barren pegmatites have been identified during recent exploration activity. These pegmatites range in thickness from <1 to >10 m and are concentrated north of the Bay d'Est Fault. They typically intrude into felsic volcanic tuffs and schists of the Dolman Cove Formation but are also recorded cutting the peraluminous Peter Snout and Rose Blanche granites. Where the margins of the dykes are observed, they cut the S_1 schistosity in the host rocks, and some pegmatites appear to pinch and swell along strike, similar to the boudinaged pegmatite dyke observed at the Killick pegmatite field (Conliffe *et al.*, 2024). Both zoned and unzoned Li-barren pegmatites have been identified, with most pegmatites unzoned, and coarse to medium grained (Plate 1A). Zoned pegmatites typically have a finer grained margin with abundant albite and thin (<2 mm) trails of garnet running parallel to the dyke margins (Plate 1B).

Samples were collected from a representative suite of Li-barren pegmatites in the Peter Snout area (Figure 2). These include samples located near Li-enriched pegmatites at the Killick pegmatite field (sample 23JC013A01) and the Hydra pegmatite (sample 23JC023A01), samples that intruded the Dolman Cove Formation and the Peter Snout and Rose Blanche granites away from known mineralized dykes, and a single sample from ~15 km west of the Killick pegmatite field associated with a small peraluminous granite similar to the Peter Snout Granite (sample 22JC117B01).

MINERALOGY OF PEGMATITES

Li-barren pegmatites in the Peter Snout area are composed of variable proportions of plagioclase (20–50%), quartz (20–40%), K-feldspar (5–30%), muscovite (5–30%) and garnet (1–5%). Some pegmatites also include large (up to 10 cm) euhedral beryl crystals (Plate 1C), but the distribution of these crystals is somewhat erratic. Tourmaline is not recorded in these dykes, but abundant tourmaline–quartz–pyrite-veining occurs in the host rocks close to the dykes, particularly near the fault zone. In the finer grained margins of zoned pegmatites, plagioclase and quartz are the major mineral present (>90% of total modal mineralogy), with minor garnet and muscovite. Molybdenite has also been recorded in some pegmatite dykes, forming large rosettes (up to 1 cm) or occurring as disseminations in finer grained areas of the dykes.

Plagioclase occurs as both large primary crystals (commonly moderately altered to sericite) or as fine-grained patches intergrown with quartz ± garnet (Plate 1D). Plagioclase locally develops myrmekitic texture, particularly when in contact with K-feldspar (Plate 1E). Quartz is typically anhedral, filling space between earlier crystallized minerals or with fine-grained plagioclase. K-feldspar forms large crystals (up to a few cm) and commonly displays plagioclase exsolution or forms graphic intergrowths with quartz, crosshatch twinning is also recorded (Plate 1E). Muscovite is mostly pale-green and typically forms large crystals (up to 2 cm), but some patches of finer grained (presumably secondary) muscovite are also recorded. Larger muscovite grains display deformation features, with warped or bent cleavage planes (Plate 1F), and some muscovite grains contain inclusions of garnet or quartz (Plate 1A).

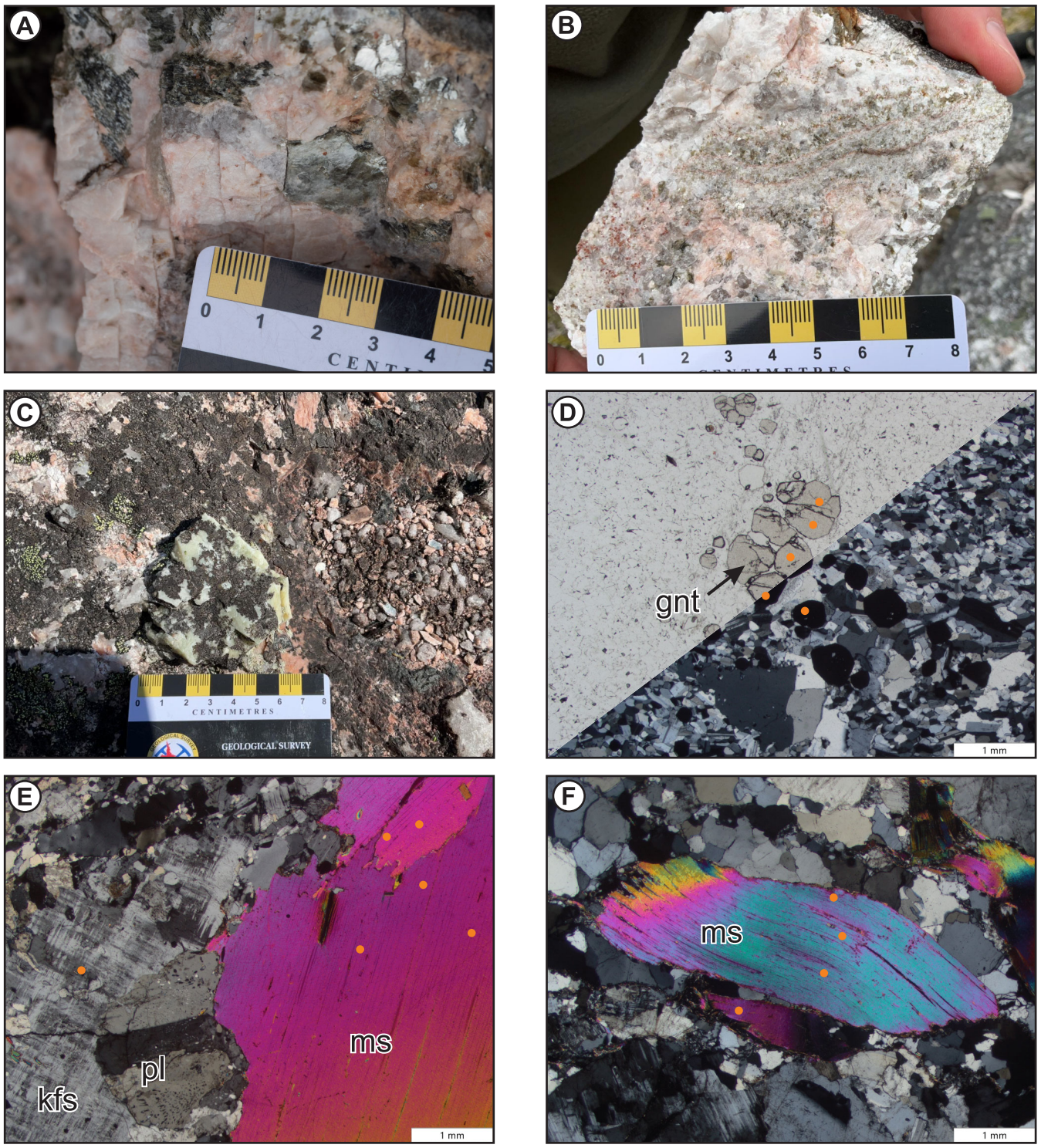

Plate 1. *Representative field photographs and photomicrographs from pegmatites in the Peter Snout area. A) Typical Li-barren pegmatite with K-feldspar, quartz, muscovite and garnet; B) Fine-grained pegmatite from close to margin of zoned Li-barren pegmatite, with layering defined by trail of small garnets; C) Large euhedral green beryl in unzoned Li-barren pegmatite; D) Fine-grained pegmatite with quartz, albite and larger, euhedral to subhedral garnet (ppl and xp); E) Typical coarse-grained pegmatite, with K-feldspar (microcline), muscovite, plagioclase (with myrmekitic texture) and quartz (xp); F) Deformed muscovite grain (xp);*

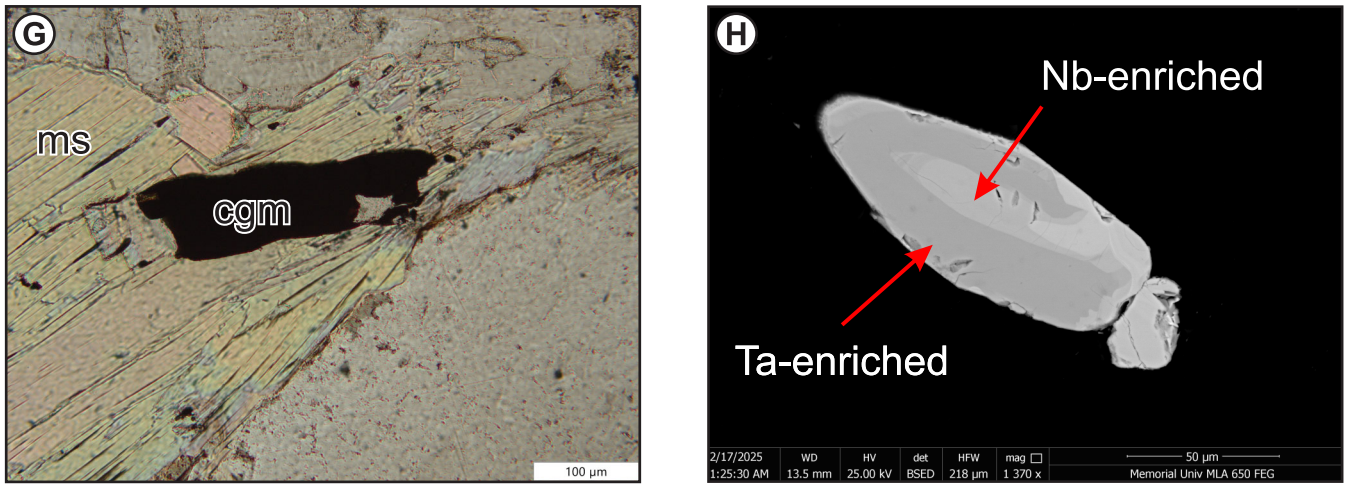

Plate 1 (Continued). *G) Large CGM grain on margin of muscovite grain (ppl); H) Zoned CGM grain with Ta rich rim and Nb-rich core (BSE). Orange spots mark location of EPMA and LA-ICP-MS analyses. Mineral abbreviations after Whitney and Evans (2010).*

Garnet forms euhedral grains up to 5 mm, which are typically fractured and most commonly occur with fine-grained plagioclase and quartz.

The main accessory minerals observed in Li-barren pegmatites from the Peter Snout area are apatite, columbite-group minerals (CGM) and zircon. Apatite occurs as sub- to anhedral pale-green crystals up to 500 µm. The CGM were observed in all samples, and form elongate euhedral to subhedral crystals up to 200-µm long (Plate 1G). They display distinct zoning in backscatter electron (BSE) images, with brighter Ta and darker Nb enriched zones (Plate 1H). The CGM are most common in finer grained, plagioclase rich parts of the pegmatites, and have been observed as inclusions in garnet crystals. Zircon forms subhedral to anhedral crystals with erratic Hf and U rich zoning. Other rare accessory minerals found in some samples include titanite, monazite and scheelite. Sample 22JC017B0, also contains a number of small (<50 µm) cassiterite grains intergrown with CGM.

PEGMATITES IN THE SNOWSHOE POND AREA

Two large pegmatite bodies in the Snowshoe Pond area (NTS 12A/7) intrude metasedimentary rocks of the Spruce Brook Formation (Figure 3). The southern pegmatite body is exposed in a northeast trending series of outcrops over ~3 km of strike length southeast of the Ebbegunbaeg Road, while a smaller northern pegmatite occurs approximately 1km north along the road. These pegmatites were first reported by Colman Sadd (1987a) during a regional bedrock mapping project, and the northernmost of these pegmatite bodies was described by Magyarosi (2020), who classified them as LCT-type pegmatites based on their mineralogy and geochemistry.

The Snowshoe Pond area is located in the Meelpaeg subzone of the Gander Zone, and the local geology has been described by Magyarosi (2020). The pegmatites are posttectonic and intruded metasediments and amphibolites of the Spruce Brook Formation (Colman-Sadd, 1987a). These metasedimentary rocks were metamorphosed to upper-

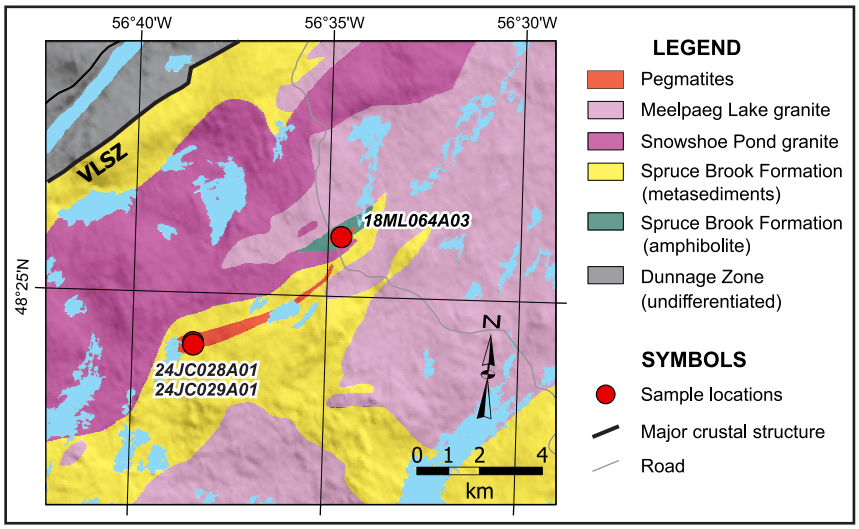

Figure 3. *Geological map of the Snowshoe Pond area, showing main geological units and sample locations. Adapted from Colman-Sadd (1987b). VLSZ–Valentine Lake Shear Zone.*

amphibolite facies and are locally partially melted to form migmatites (Colman-Sadd, 1987a; Valverde-Vaquero *et al.*, 2006). This anatexis is interpreted to have occurred during peak metamorphism in the Ordovician (Valverde-Vaquero *et al.*, 2006). The Spruce Brook Formation is intruded by a number of granites, including the Ordovician Snowshoe Pond Granite (Valverde-Vaquero *et al.*, 2006), and the Silurian Meelpaeg Lake Granite (part of the North Bay Granite Suite; Dickson, 1990). Magyarosi (2020) reported that no suitable fertile parent granites for LCT-type pegmatites occur within 10 km of these pegmatites, and it is uncertain if their origin is related to anatexis or fractionation from an unexposed parent granite at depth.

The southern pegmatite forms a large composite body up to 500-m wide and 5-km in length. It is well exposed at its southern end and varies from very coarse-grained pegmatite to medium-grained granite. No internal zoning of the pegmatites was observed, but pegmatitic zones are observed to have gradational contacts with granitic phases. The pegmatitic phases are characterized by well-developed graphic intergrowths of K-feldspar and quartz (Plate 2A) and spectacular patches of plumose silvery muscovite up to 50-cm in diameter (Plate 2B-C). The northern pegmatite, which is well exposed in a roadcut along the Ebbegunbaeg Road, intrudes amphibolites of the Spruce Brook Formation. It has similar textures to the southern pegmatite, with well-developed graphic textures, plumose muscovite and fine- to medium-grained aplitic patches (Magyarosi, 2020), but no granitic phases have been observed in this pegmatite. The northern pegmatite also has some more evolved characteristics, including light-green rather than silver muscovite (Plate 2D) and the presence of accessory tourmaline and CGM (Magyarosi, 2020).

Two samples of the southern pegmatite were collected for petrographic and mineral chemistry studies. In addition, a suite of samples from the northern pegmatite, previously described by Magyarosi (2020), were examined and one sample (18ML064A03) was selected for mineral chemistry analysis.

MINERALOGY OF PEGMATITES

No Li minerals were recorded in samples from the northern or southern pegmatites, and they are therefore classified as Li-barren pegmatites. The following descriptions are a combination of observations recorded during this study from the southern pegmatite and those by Magyarosi (2020) from the northern pegmatite. As the mineralogy and textures are similar from both areas, they are described together unless noted. The modal mineralogy of the pegmatites is variable but typically comprises of quartz (20–40%), plagioclase (20–40%), K-feldspar (10–30%), muscovite (5–30%, garnet (0–10%) and biotite (0–5%). Rare beryl has also been recorded in both pegmatites, but its distribution is erratic. Accessory minerals observed include apatite, magnetite and zircon, and Magyarosi (2020) also reported on the presence of tourmaline, monazite, xenotime, pyrite, gahnite and CGM in the northern pegmatite.

K-feldspar commonly occurs as grains with crosshatch twining (Plate 2E, F) and local perthitic textures or as graphic intergrowths with quartz (Plate 2G). Plagioclase occurs both as large grains or in fine-grained sections with quartz and muscovite. Both feldspars are weakly to moderately altered to sericite or saussurite, respectively. Muscovite ranges from colourless to green and pink in plane-polarized light, and occurs as large, weakly deformed grains (Plate 2E, F), in fine-grained sections or as plumose laths with symplectic intergrowths of muscovite and quartz (Plate 2H). Garnet occurs as euhedral to subhedral grains, weakly zoned in some samples and commonly fractured (Plate 2E). Biotite occurs as radiating bladed sheets and is weakly altered to chlorite in some samples. Beryl, where present, forms subhedral to anhedral crystals (up to 10 cm) and is light to blueish green.

PEGMATITES IN THE CAPE FREELS AREA

Pegmatites in the Cape Freels area were first reported by Tater (1964) and described in detail by Gale (1966, 1967). This work followed the Bonavista North fire in 1961, which resulted in excellent exposure, and subsequent fieldwork during the present study noted that many of the pegmatites described by Gale (1966, 1967) have extensive lichen and vegetation cover. Therefore, the descriptions of the pegmatites are mostly based on the original descriptions of Gale (1966, 1967).

The largest concentration of pegmatites in the Cape Freels area is located in the New-Wes-Valley area, but similar pegmatites have been reported from across the study area. The oldest rocks are metasedimentary rocks of the Gander Group and high-grade metamorphic rocks of the Hare Bay Gneiss (Langille, 2012). Langille (2012) showed that the Hare Bay Gneiss was not simply a metamorphic equivalent of the Gander Group but appears to be a distinct metasedimentary unit that underwent significant metamorphism and anatexis during the Penobscot orogeny (*ca.* 465–460 Ma). The Gander Group and Hare Bay Gneiss were intruded by multiple syn- to posttectonic granitic plutons, which represent multiple phases of syn- to posttectonic Silurian and Devonian granitic magmatism (Wang *et al.*, 2024). This includes a number of peraluminous two-mica and locally garnet-bearing granites, including the Business Cove Granite and numerous unnamed granite bodies (Jayasinghe, 1978).

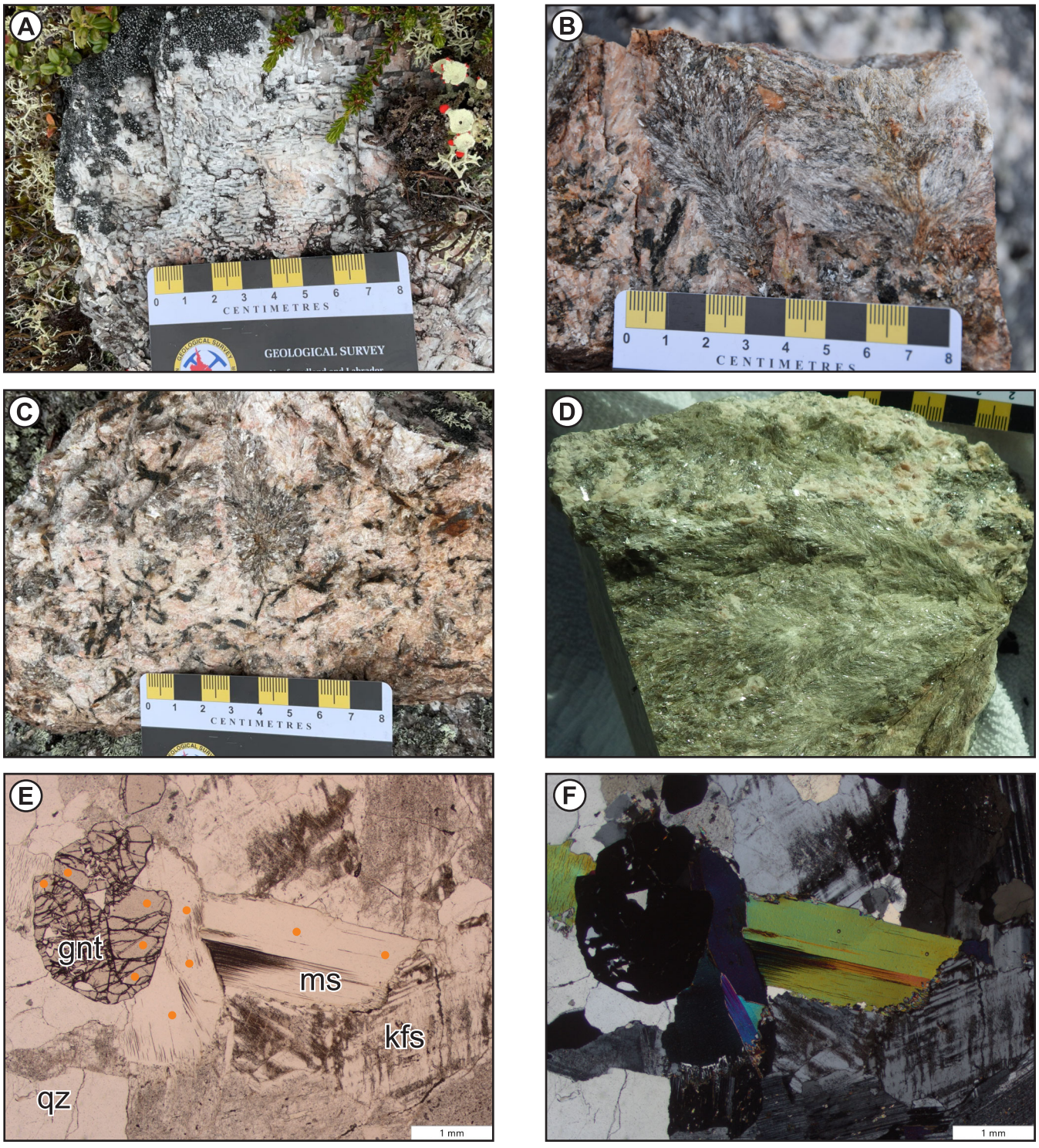

Plate 2. *Representative field photographs and photomicrographs from pegmatites in the Snowshoe Pond area. A) Symplectic intergrowth of K-feldspar and quartz, southern pegmatite; B) Plumose aggregates of silver-coloured muscovite, southern pegmatite; C) Plumose silver-coloured muscovite and acicular biotite crystals, southern pegmatite; D) Plumose green muscovite, northern pegmatite; E) Typical coarse-grained pegmatite with muscovite, garnet, K-feldspar (microcline) and quartz (ppl); F) Same view as E), in xp.*

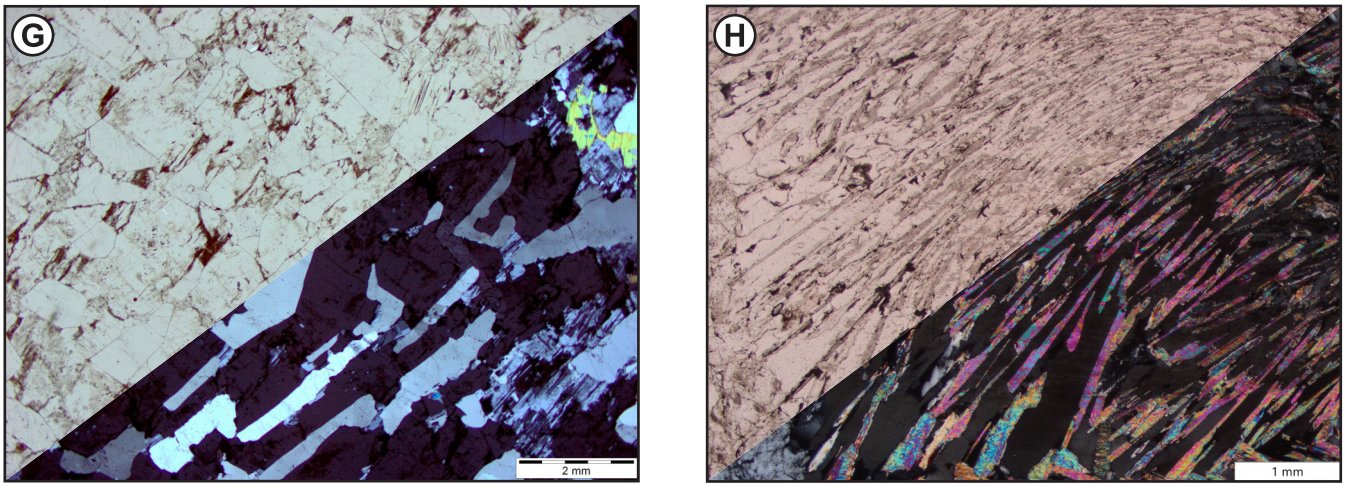

Plate 2 (Continued). *G) Graphic intergrowth of K-feldspar and quartz (ppl and xp); H) Plumose muscovite, with elongate muscovite crystals and interstitial quartz (ppl and xp). Orange spots mark location of EPMA and LA-ICP-MS analyses. Mineral abbreviations after Whitney and Evans (2010).*

The Dover Fault, a major crustal structure, which represents the boundary between Ganderia and Avalonia, is located directly east of the study area (Figure 4).

Gale (1966) identified more than 125 individual pegmatites over an area of ~15 km^2, 8 km west of New-Wes-Valley. These pegmatites are up to 6-m thick (typically 0.5 to 1 m thick) and some can be traced along strike for more than 100 m. These pegmatites intrude both the Business Cove Granite and the surrounding Hare Bay Gneiss and were subdivided by Gale (1966) into "simple" and "complex" pegmatites, based on mineralogy and zoning. Simple pegmatites consist of K-feldspar, quartz and plagioclase with lesser muscovite and garnet and rare tourmaline and garnet. Complex pegmatites have well defined zoning, with a fine- to very fine-grained border zone composed of plagioclase, quartz and garnet, a medium-grained intermediate zone with K-feldspar, quartz, muscovite, plagioclase, garnet and tourmaline (Plate 3A), and a core zone of quartz ± beryl ± chrysoberyl (Plate 3B). No Li-minerals were observed, so all the pegmatites are classified as Li-barren. Similar, but less abundant, pegmatites that were recorded throughout the area between Cape Freels and Hare Bay intruded all the rock units. Langille (2012) reported a U–Pb zircon age of 387 ± 2 Ma from a pegmatite in Windmill Bight Provincial Park, but it is unknown if this represents the age of all pegmatites in this area.

Other zones of pegmatites were recorded during regional bedrock mapping campaigns. The Ocean Pond pegmatite field was described by O'Neill (1991). It occurs east of the peraluminous, muscovite–garnet-bearing Ocean Pond Granite (Figure 4), where abundant granite and pegmatite sheets (approximately 25% of the total outcrop) intruded metasedimentary rocks of the Gander Group over an area ~10 x 1 km (Plate 3C). The pegmatites are medium to coarse grained and have a weak zonation with finer grained border zones. The mineralogy comprises of abundant green muscovite, K-feldspar, quartz, plagioclase, garnet and tourmaline, with beryl in some pegmatites. These pegmatites typically have a well-developed schistosity. Another area of abundant pegmatites is located east of Gambo Pond, where sheets of peraluminous, garnet-bearing granites and garnet–tourmaline-bearing pegmatites intrude metasedimentary rocks of the Gander Group (O'Neill, 1992).

Samples were collected from three areas (Figure 4), three samples from the New-Wes-Valley area, one from the Oceans Pond area and one from east of Gambo Lake.

MINERALOGY OF PEGMATITES

The pegmatites in the Cape Freels area have a highly variable mineralogy and textures depending on sample location and zoning in individual pegmatite bodies. However, they predominantly consist of K-feldspar, quartz, plagioclase and muscovite (observed in all samples), with some pegmatites also containing significant garnet, tourmaline and rare biotite, beryl and chrysoberyl. Accessory minerals include apatite, zircon, titanite and monazite, however, no CGM were observed. The following is a general description of the minerals observed in the five selected samples.

K-feldspar forms large grains with crosshatch twinning and in some samples, it has a well-developed perthite texture with plagioclase exsolutions (Plate 3D). Plagioclase occurs as large grains with well developed twinning, or in finer grained patches with quartz and muscovite (± garnet). Both feldspars are weakly to moderately altered to sericite or saussurite, respectively. Muscovite typically occurs as

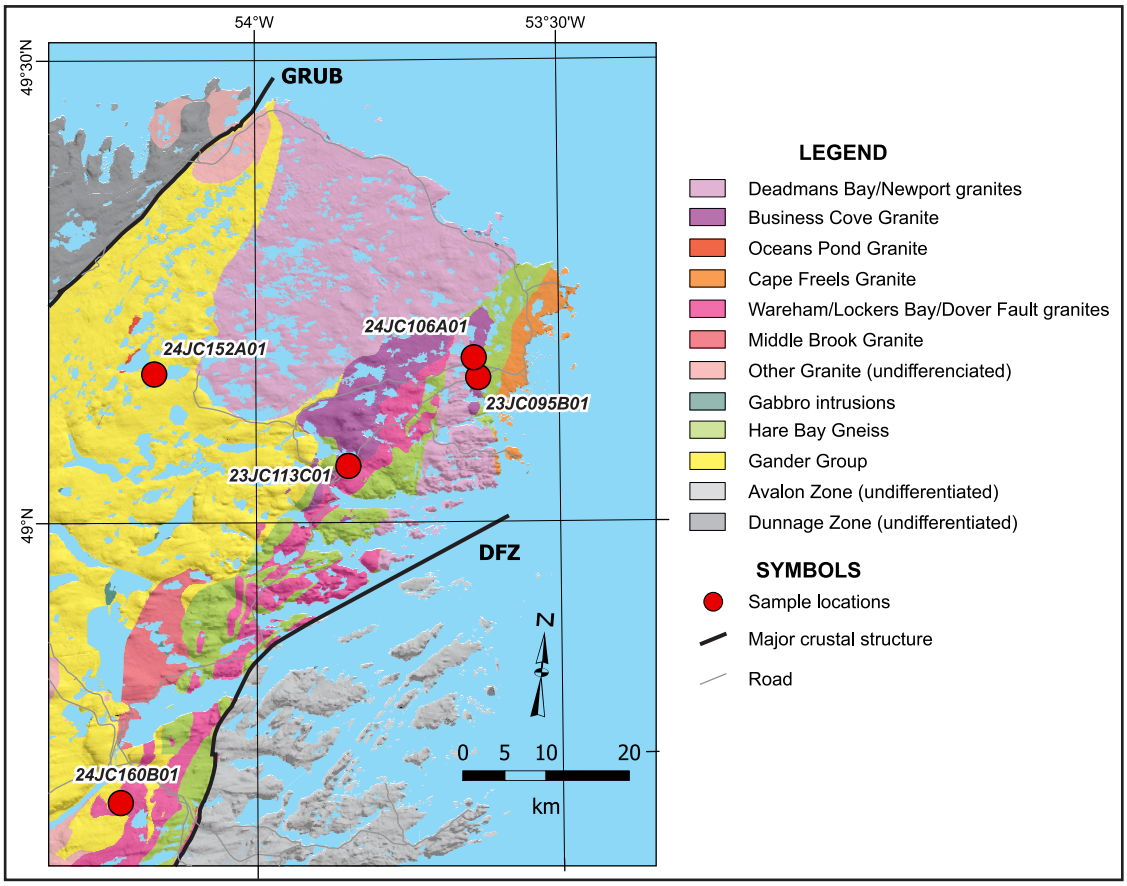

Figure 4. *Geological map of the Cape Freels area, showing main geological units and sample locations. Adapted from Jayasinghe (1978), Meyer* et al. *(1984), O'Brien* et al.*, (1987) and O'Neill (1990). DFZ–Dover Fault Zone, GRUB–Gander River Ultramafic Belt.*

large grains with mottled extinction (Plate 3D–F), secondary fine-grained muscovite is also observed (Plate 3D). Garnet forms euhedral to subhedral grains (Plate 3F) and is commonly fractured and occasionally pseudomorphed by secondary muscovite. Tourmaline, where present, is zoned with dark rims and light cores (Plate 3G). BSE imaging of zircons in sample 24JC160B01 show that they are typically anhedral and erratically zoned (Plate 3H), characteristic of zircons crystallized during the magmatic-hydrothermal transition (Esteves *et al.*, 2025).

MINERAL CHEMISTRY

The EPMA and LA-ICP-MS data were collected from plagioclase, K-feldspar, muscovite, biotite, garnet, tourmaline and beryl in 18 samples from the three study areas (Table 1). In total, 793 EPMA and 379 LA-ICP-MS analyses were collected, and with mineral chemistry data summarized in the supplementary tables. These data are discussed below, organized by mineral type. The results from each study area (Peter Snout, Snowshoe Pond and Cape Freels) have been combined unless individual samples have anomalous values. An exception has been made for K-feldspar and muscovite from sample 22JC117B01, which is located ~15 km west of the other samples from the Peter Snout area, and has very different geochemical characteristics.

PLAGIOCLASE

The EPMA data was collected from plagioclase in all samples (n = 198), with LA-ICP-MS data collected from four samples (n = 19) due to the poor ablation of plagioclase grains. The EPMA data show that plagioclase from the Burgeo area ranges from albite to oligoclase in composition (Ab_{71} to Ab_{100}), whilst plagioclase from the Snowshoe Pond and Cape Freels areas is albite in composition (Ab_{91} to Ab_{100}; Figure 5A–C), with the oligoclase compositions corresponding to higher Ca values (up to 6.47 wt. % CaO; Figure 5D).

Trace-element contents are low (<100 ppm) in all samples, but limited data indicates that samples from the Burgeo area are relatively enriched in Li, Be, Ga, Rb, Cs, Pb and total REE.

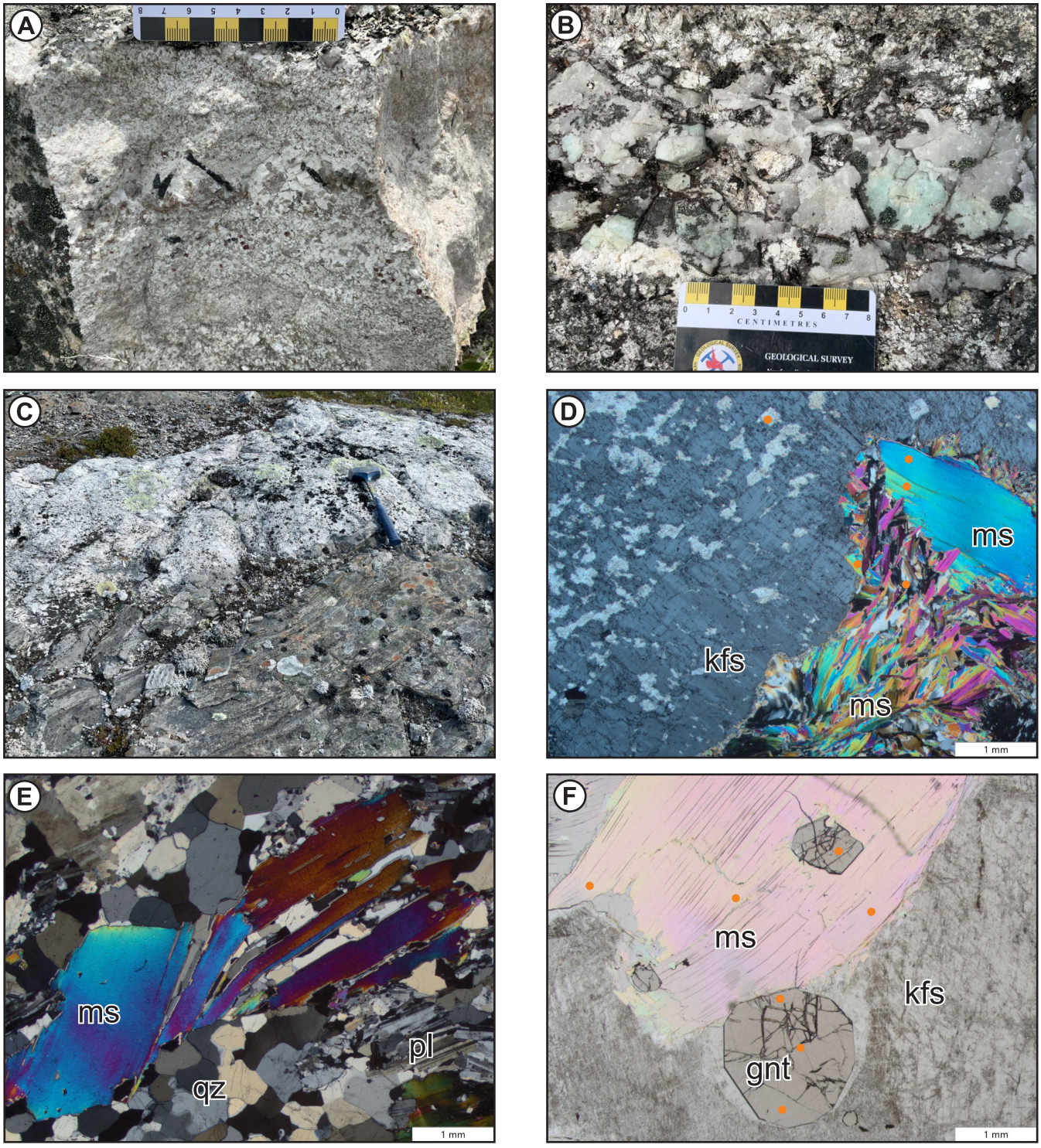

Plate 3. *Representative field photographs and photomicrographs from pegmatites in Cape Freels area. A) Zoned pegmatite with coarse and fine grained layers and elongate tourmaline crystals; B) Core of zoned pegmatite, with quartz and light green beryl; C) Pegmatite crosscutting foliation in deformed metasediments of the Gander Group; D) Microcline with perthite texture, and two generations of muscovite (xpl); E) Typical medium-grained pegmatite with muscovite, quartz and plagioclase (xpl); F) Coarse-grained pegmatite with muscovite (deformed), garnet and K-feldspar (ppl);*

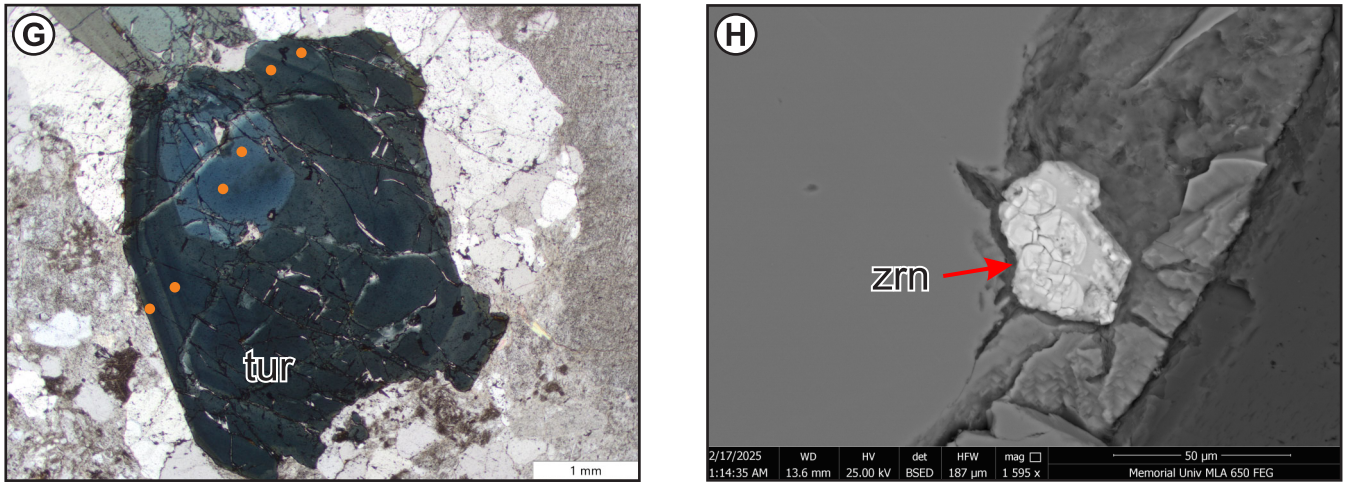

Plate 3 (Continued). *G) Zoned tourmaline with dark blue rim and light blue core (ppl); H) Anhedral, erratically zoned zircon (BSE). Orange spots mark location of EPMA and LA-ICP-MS analyses. Mineral abbreviations after Whitney and Evans (2010).*

K-FELDSPAR

The K-feldspar EMPA data was collected in 11 samples (n = 99), with LA-ICP-MS data only collected from five samples due to poor ablation of K-feldspar grains (n = 24). All analyzed grains are slightly sodic in composition of Or_{84} to Or_{96} (Figure 5A–C), corresponding to 0.31 to 1.40 wt. % Na_2O. Based on its major-element chemistry and petrographic characteristics, K-feldspar is classified as microcline.

Trace-element data shows significant variations between samples from different study areas. Apart from sample 22JC117B01, microcline from the Burgeo area is strongly enriched in Li, B, Ga, Rb and Cs and has lower K/Rb ratios (Figure 5E, F). In particular, microcline in sample 25JC008B01, located north of the Killick Pegmatite field cutting the peraluminous Peter Snout granite, is strongly elevated in Li (up to 237 ppm).

MUSCOVITE

Major- and trace-element data from muscovite was collected in all samples, with 311 EPMA analyses and 202 LA-ICP-MS analyses. In the mica classification diagram of Tischendorf *et al.* (2004), muscovite has phengite to Li-phengite compositions (Figure 6A).

Trace-element data from muscovite shows significant variations between the sampled study areas. Samples from the Peter Snout area (excluding sample 22JC117B01) are strongly enriched in Rb (up to 7740 ppm), Cs (up to 4130 ppm), Ga (up to 411 ppm), Zn (up to 1540 ppm) and Nb (up to 581 ppm) and have slightly elevated Be, B, Ta and Pb contents compared to muscovite from other areas. Muscovites from the Peter Snout area also have lower K/Rb (9.1 ± 3.7) than muscovite from the Cape Freels (27.1 ± 12.5) and Snowshoe Pond (32.3 ± 6.0) areas, and there is a strong negative correlation between K/Rb and Cs and Ga contents of muscovite (Figure 6B, C). The Li and Sn contents are highly variable between samples, and there is no correlation between Li and Sn contents and K/Rb (Figure 6D). Sample 22JC117B01 is also characterized by elevated Sn values (up to 1720 ppm). Rb/Cs ratios show that samples from the Peter Snout area have depleted Rb/Cs compared to other areas (Figure 6E).

BIOTITE

Biotite was analyzed in one sample from the Snowshoe Pond area, with five EPMA and five LA-ICP-MS analyses. Biotite plots in the Mg–Fe field in the mica classification diagram of Tischendorf *et al.* (2004), close to the annite node (Figure 6A). Trace-element data from biotite show that they have high Li (up to 1570 ppm), Zn (up to 2740 ppm) and Ga (up to 139 ppm) contents with some analyses having elevated Nb (up to 650 ppm) and Ta (up to 106 ppm).

GARNET

Garnet is an accessory phase in all pegmatites, and a total of 112 EPMA and 76 LA-ICP-MS analyses were collected. Garnet from the Peter Snout area is predominantly spessartine in composition (Sp_{60-70}, Alm_{25-40}), with samples from the Snowshoe Pond area more almandine in composition (Sp_{35-40}, Alm_{55-60}). Garnets from the Cape Freels area show a wide range of compositions (Figure 7A), ranging from spessartine (>Sp_{65}) to almandine-rich (>Alm_{60}).

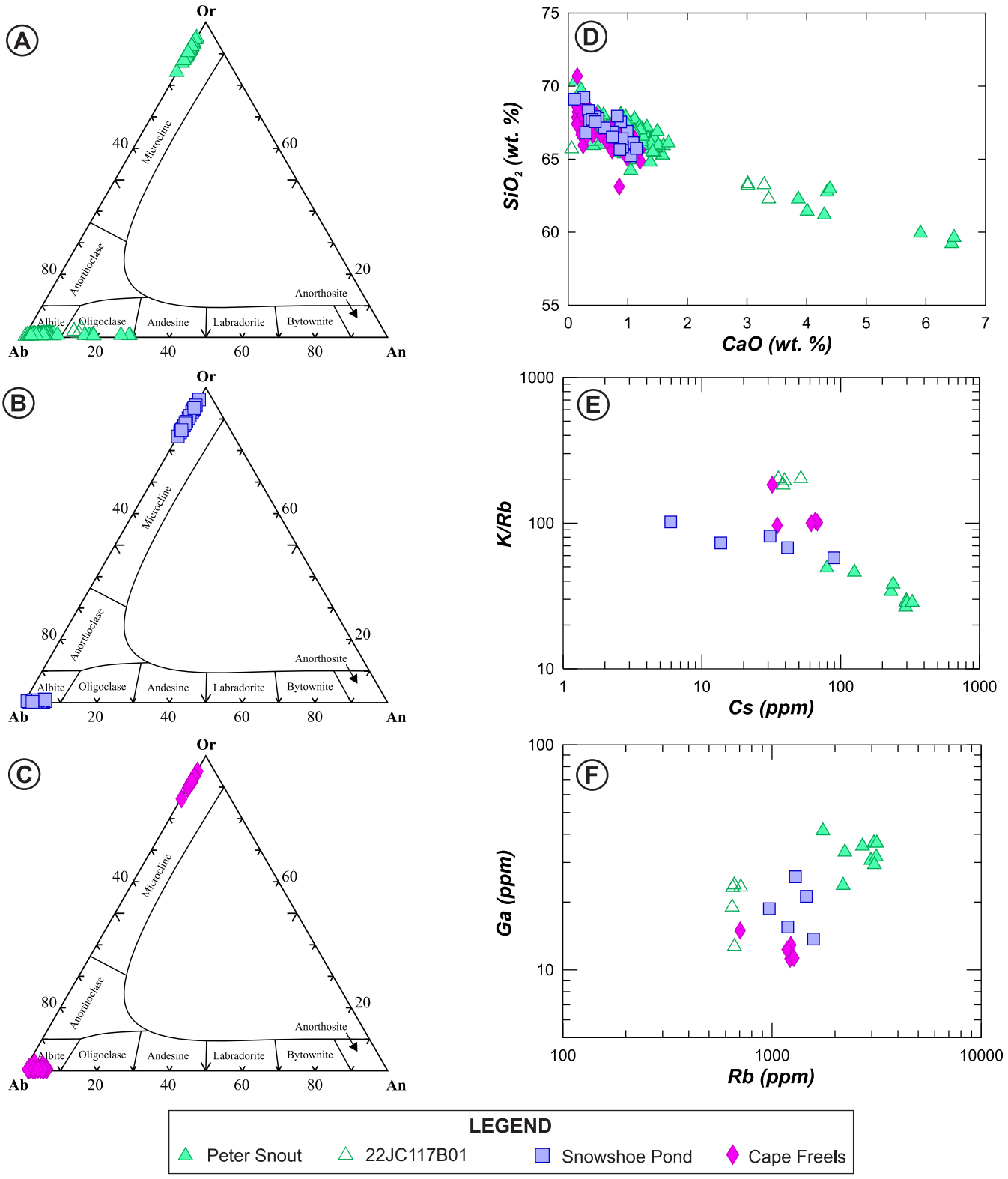

Figure 5. *Classification and mineral chemistry diagrams for the plagioclase and K-feldspar. A) Feldspar classification diagram (after Deer* et al.*, 1992) for plagioclase and K-feldspar in the Peter Snout area; B) Feldspar classification diagram (after Deer* et al.*, 1992) for plagioclase and K-feldspar in the Snowshoe Pond area; C) Feldspar classification diagram (after Deer* et al.*, 1992) for plagioclase and K-feldspar in the Cape Freels area; D) Bivariate plot of* SiO_2 vs. *CaO for plagioclase; E) K-feldspar K/Rb* vs. *Cs plot; F) Bivariate plot of Ga* vs. *Rb for K-feldspar.*

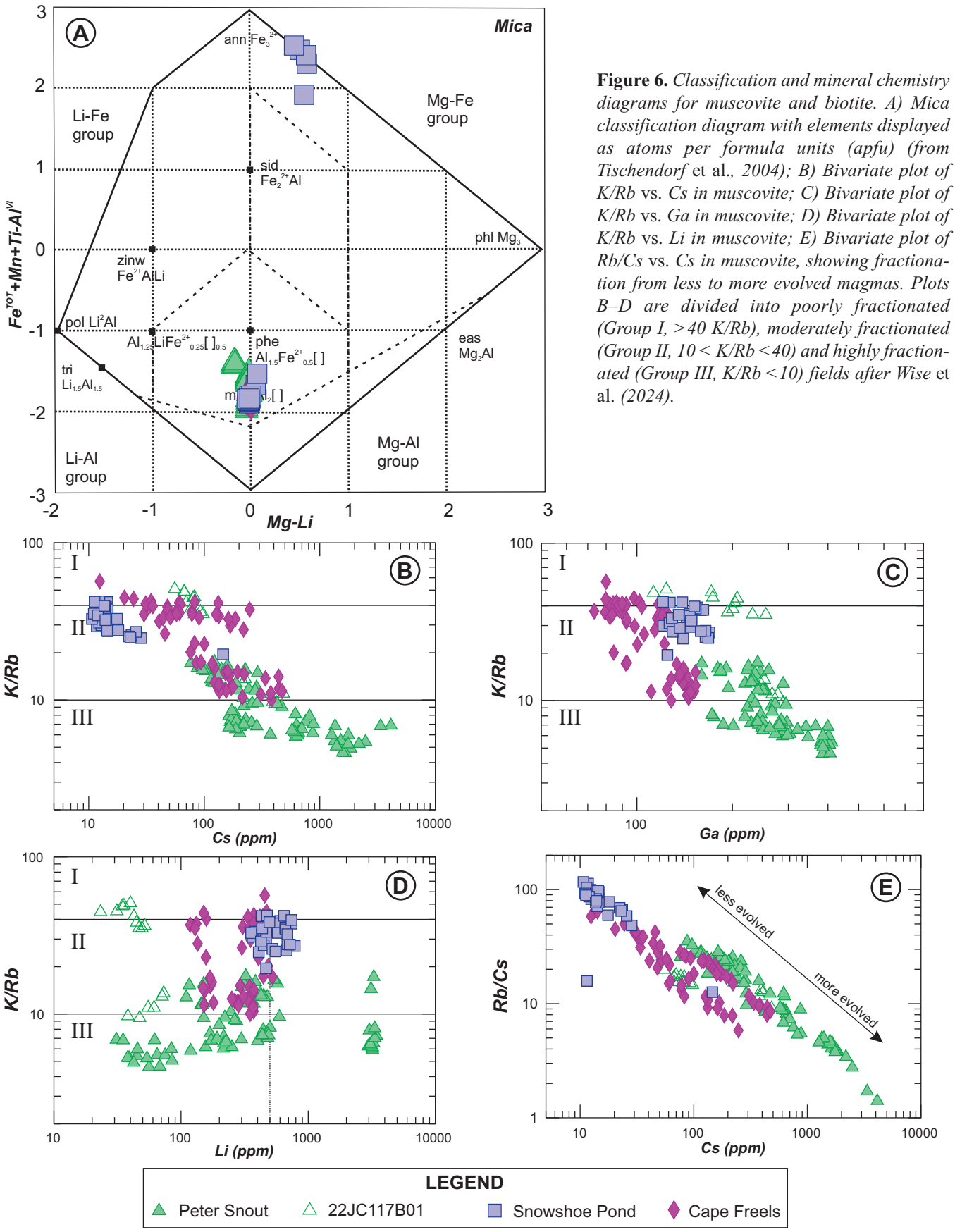

Figure 6. *Classification and mineral chemistry diagrams for muscovite and biotite. A) Mica classification diagram with elements displayed as atoms per formula units (apfu) (from Tischendorf* et al.*, 2004); B) Bivariate plot of K/Rb* vs. *Cs in muscovite; C) Bivariate plot of K/Rb* vs. *Ga in muscovite; D) Bivariate plot of K/Rb* vs. *Li in muscovite; E) Bivariate plot of Rb/Cs* vs. *Cs in muscovite, showing fractionation from less to more evolved magmas. Plots B–D are divided into poorly fractionated (Group I, >40 K/Rb), moderately fractionated (Group II, 10 < K/Rb <40) and highly fractionated (Group III, K/Rb <10) fields after Wise* et al. *(2024).*

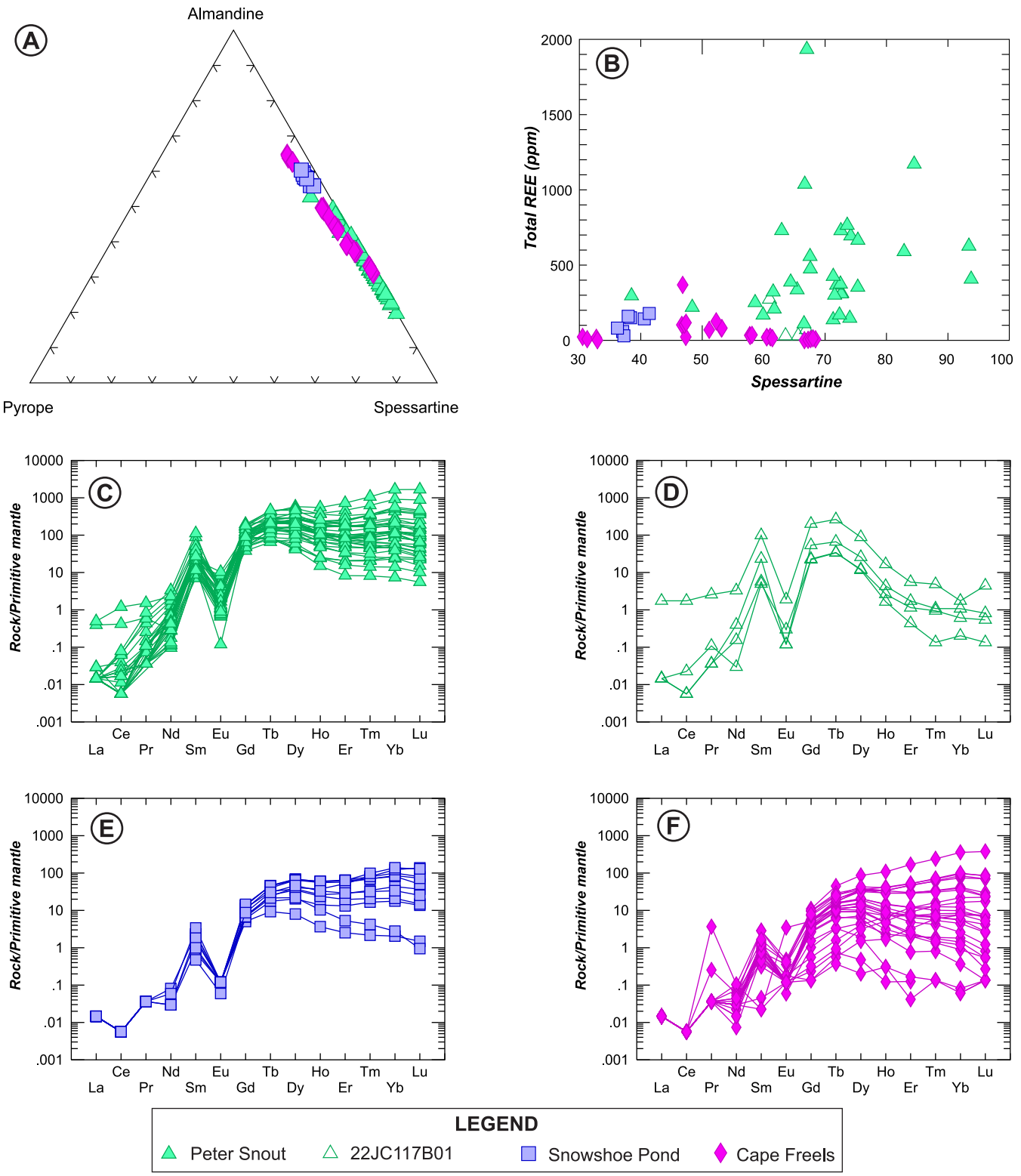

Figure 7. *Classification and mineral chemistry diagrams for garnet from the three study areas. A) Garnet classification diagram with end members; pyrope ($Mg_3Al_2Si_3O_{12}$), almandine ($Fe_3Al_2Si_3O_{12}$) and spessartine ($Mn_3Al_3Si_3O_{12}$); B) Total rare-earth content* vs. *spessartine content of garnet; C–F) Chondrite-normalized REE diagrams plotting garnet REE data. Normalizing values from Sun and McDonough (1989).*

Trace-element data show that garnet from all the areas have similar Li, Ga, Zn and Cs contents, with no significant variations observed. Garnet from the Peter Snout area are enriched in Nb and Ta and have total rare-earth-element (ΣREE) contents of 468 ± 368 ppm, significantly higher than ΣREE from the Cape Freels and Snowshoe Pond areas (Figure 7B). There is also a strong correlation between ΣREE and garnet compositions, with the highest ΣREE contents in spessartine garnets (>Sp_{60}). Garnet is typically enriched in heavy-rare-earth elements (HREE), with light-rare-earth elements (LREE) typically at or below detection limits. Rare-earth element profiles for garnet highlight the strong depletion in LREE compared to HREE in some garnets, as well as a strong negative Eu anomaly (Figure 7D–G).

TOURMALINE

Mineral chemistry data were collected from tourmaline in the wall-rock of a pegmatite in the Peter Snout area (sample 23JC013A01), and two samples of tourmaline-bearing pegmatites in the Cape Freels area. In total, 46 EPMA and 24 LA-ICP-MS analyses were collected from tourmaline.

Tourmaline in the wallrock of pegmatites in the Peter Snout area are alkali (according to classification of Henry *et al.*, 2011; Figure 8A), with Na and Ca dominant (K_2O < 0.05 wt. %). In the dravite–schorl–elbaite (Mg–Fe–Li + Al) ternary system, tourmaline ranges from schorl to dravite in composition (Figure 8B). Li contents are low (<300 ppm), but some grains show enrichment in Co (up to 171 ppm), Nb (up to 114 ppm) and Ta (up to 350 ppm).

Tourmaline in the Cape Freels area has lower Ca contents (CaO < 0.2 wt. %) with Na the dominant alkali element and is classified as dravite (Figure 8B), with transects across zoned tourmaline showing that the rims are relatively enriched in Na_2O and TiO_2, and corresponding decreases in X-site vacancy. Trace-element concentrations in tourmaline show low Li (<120 ppm), with Zn ranging from 793 to 1492 ppm and Sn from 9 to 24 ppm.

BERYL

Beryl was analyzed in three samples from the Peter Snout area, with a total of 22 EPMA and 29 La-ICP-MS analyses. Beryl is strongly enriched in Li (2445 ± 1297 ppm) and Cs (2286 ± 722 ppm), with elevated Zn (average 472 ppm) and Rb (111 ppm).

DISCUSSION

The data collected show that the mineralogy and mineral chemistry of Li-barren pegmatites is variable depending on whether the pegmatites are spatially associated with known Li-enriched pegmatites (Peter Snout area) or are located in areas with no known Li-enriched pegmatites (Snowshoe Pond and Cape Freels areas). In addition, sample 22JC117B01 from the Peter Snout area, which is located the farthest from known Li-enriched pegmatites (Figure 2) has distinct mineral chemistry from other pegmatites in the Peter Snout area. This suggests that detailed petrographic and mineral-chemistry studies of the much more abundant Li-barren pegmatites have the ability to assess the potential of an area to host Li-enriched pegmatites, which typically have a much smaller spatial footprint.

The major mineralogy of pegmatites in all three areas is broadly similar, with abundant quartz, K-feldspar (micro-

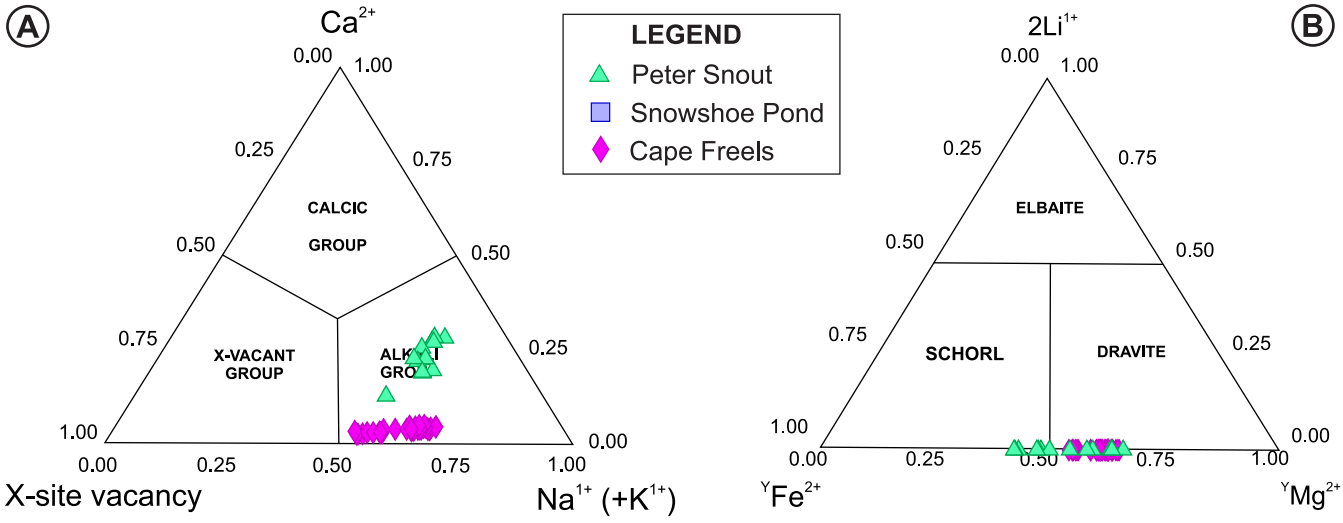

Figure 8. *Tourmaline primary group and species classification based on the occupancy in the A) X-, and B) Y-sites (Henry* et al.*, 2011).*

cline), plagioclase (albite), muscovite and garnet, with biotite, tourmaline and beryl also recorded. The CGM are common in Li-barren pegmatites in the Peter Snout area but are rare or absent in pegmatites from the Snowshoe Pond and Cape Freels area, suggesting that the recognition of these minerals is indicative of a high potential for LCT pegmatite mineralization.

Muscovite was analyzed in all samples, and previous studies have shown that muscovite is an excellent indicator of magmatic fractionation and mineral potential (Maneta and Baker, 2019; Wise *et al.*, 2024, van Lichtervelde *et al.*, 2025), due to the ability for Rb, Cs and Li to substitute for K in the mica structure. Trace-element data from Li-barren pegmatites in the Peter Snout area show that muscovite has low K/Rb ratios (<20) and fall in the fields of moderately to highly fractionated pegmatites (Wise *et al.*, 2024; Figure 6B–D). Muscovite in pegmatites from the Snowshoe Pond and Cape Freels area have higher K/Rb ratios and generally fall in the field of moderately fractionated pegmatites (Wise *et al.*, 2024; Figure 6B–D). The muscovite data from pegmatites in the Peter Snout area also show elevated Cs and Ga values (Figure 6B, C), with the highest Cs values (>1000 ppm) in a Li-barren pegmatite ~5 m above the pollucite-bearing Hydra pegmatite, and muscovite from all areas show clear Rayleigh-type fractionation trends to more evolved, Cs-rich compositions (Figure 6E; van Lichtervelde *et al.*, 2025). Li contents in muscovite are highly variable, ranging from <50 to >3000 ppm, and do not show any correlation with K/Rb (Figure 6D). The K/Rb-Li plot for muscovite from all areas (Figure 6D) show that these data overlap both the Li-rich and Li-poor fields as defined by Wise *et al.* (2024).

Trace-element data from K-feldspar is also a key indicator of magmatic fractionation in pegmatites, with incompatible elements such as Rb, Cs and Li incorporated into the crystal structure in more evolved pegmatites (Černý, 1994; Dias *et al.*, 2025). Data from this study show that K-feldspar in pegmatites from the Peter Snout area is relatively enriched in Rb, Cs, Li and Ga compared to K-feldspar in other two areas and has lower K/Rb (Figure 5E, F). These data are comparable to values for other known Li-enriched pegmatites (Curry *et al.*, 2025; Dias *et al.*, 2025) and suggests that K-feldspar geochemistry in Li-barren pegmatites is an important indicator of proximity to mineralized pegmatites.

Garnet trace-element geochemistry is also proposed as a potential indicator of magmatic fractionation in pegmatites, particularly the ratio of Mn and Fe, abundance of Nb, Ta, Hf and Zr, and the ratio of LREE to HREE (London, 2008; Hernández-Filiberto *et al.*, 2021; Curry *et al.*, 2025). Data from this study shows that garnets from pegmatites in the Peter Snout area have higher Mn contents (spessartine in composition), have higher Nb and Ta contents and are more enriched in HREE than garnets in the Snowshoe Pond and Cape Freels area (Figure 7). These geochemical characteristics are typical of more evolved pegmatites (London, 2008; Hernández-Filiberto *et al.*, 2021).

In summary, mineral-chemistry data from muscovite, K-feldspar and garnet indicate that Li-barren pegmatites from the Peter Snout area, where they are spatially associated with Li-enriched pegmatites, are characteristic of more evolved pegmatites when compared to Li-barren pegmatites in the Snowshoe Pond and Cape Freels areas. In addition, pegmatites in the Peter Snout area have common accessory CGM, which are absent in pegmatites from other areas. Although there is significant overlap in some mineral chemistry indicators and uncertainties in the temporal relationship between Li-barren and Li-enriched pegmatites, this suggests that mineral chemistry and mineralogy of Li-barren pegmatites is a useful indicator of mineral prospectivity, with more evolved characteristics of pegmatites indicative of proximity to Li-enriched pegmatites.

FUTURE WORK

Ongoing work on Li-barren pegmatites in Newfoundland include detailed petrographic and mineral chemistry studies of pegmatites from other areas (*e.g.*, Bay d'Espoir area), and geochronological studies of Li-barren pegmatites in the Peter Snout area. These will be compared with mineralogy, mineral chemistry and geochronology from Li-enriched pegmatites in the Peter Snout area (Killick pegmatite field and Hydra pegmatite) to better constrain magmatic evolution during the formation of these mineralized pegmatites and assess the effectiveness of studies of Li-barren pegmatites to evaluate mineral prospectivity.

In addition, the mineral chemistry obtained during this study, combined with data from Li-enriched pegmatites, will be compared with analyses obtained from handheld geochemical analyzers (portable XRF and Laser-Induced Breakdown Spectroscopy (LIBS) devices). These handheld analyzers are increasingly being used in field-exploration programs to rapidly obtain mineral chemistry data from pegmatites, and detailed comparisons between laboratory and field data and will help better optimize the use of these data and identify the most effective geochemical parameters to assess mineral potential during greenfields exploration.

ACKNOWLEDGMENTS

We would like to thank Maria O'Neill, Celeste Cunningham, Noah Slaney and Zsuzsanna Magyarosi for their able assistance during fieldwork. We are grateful to

Wanda Alward, Sebastian Kommescher and Dylan Goudie (MUN) for assistance during EPMA, LA-ICP-MS and SEM-MLA analyses, and the staff at the Geological Survey for their support and constructive discussions on critical mineral deposits in the province. In addition, the staff and management at Vinland Lithium, Benton Resources Inc. and Sokoman Minerals Corp. are thanked for their hospitality and assistance during fieldwork, and ongoing support for research. Zsuzsanna Magyarosi and John Hinchey are thanked for detailed and thoughtful reviews of earlier drafts of this paper. DBA acknowledges support for fieldwork funded by the Natural Sciences and Engineering Research Council of Canada and the Natural Resources Canada Targeted Geoscience Initiative.

REFERENCES

Bradley, D.C., McCauley, A.D. and Stillings, L.M.
2017: Mineral-deposit model for lithium–cesium–tantalum pegmatites. U.S. Geological Survey Scientific Investigations, Report 2010–5070–O, 48 pages.

Černý, P.
1991: Rare element granitic pegmatites. Part I: Anatomy and internal evolution of pegmatite deposits. Geoscience Canada, Volume 18, pages 49-67.

1994: Evolution of feldspars in granitic pegmatites. *In* Feldspars and their Reactions I. *Edited by* I. Parsons. Springer, Dordrecht, Netherlands, pages 501-540.

Chorlton, L.
1980a: Geology of the La Poile River area (11O/16), Newfoundland. Government of Newfoundland and Labrador, Department of Mines and Energy, Mineral Development Division, Report 80-03, 96 pages.

1980b: Peter Snout, west half. *In* Current Research. Government of Newfoundland and Labrador, Department of Mines and Energy, Mineral Development Division, Report 80-1, pages 62-73.

Colman-Sadd, S.P.
1987a: Geology of the Snowshoe Pond (12A/7) area, Newfoundland. *In* Report of Activities. Government of Newfoundland and Labrador, Department of Mines and Energy, Mineral Development Division, Report of Activities, pages 59-62.

1987b: Snowshoe Pond, Newfoundland. Map 87-087. Government of Newfoundland and Labrador, Department of Mines and Energy, Mineral Development Division, Open File 12A/07/0438.

Colman-Sadd, S.P., Hayes, J.P. and Knight, I.
1990: Geology of the Island of Newfoundland. Government of Newfoundland and Labrador, Department of Mines and Energy, Geological Survey Branch, Map 90-001.

Conliffe, J., Archibald, D.B. and Sparkes, B.A.
2024: Lithium–cesium–tantalum (LCT) pegmatites in southwestern Newfoundland. *In* Current Research. Government of Newfoundland and Labrador, Department of Industry, Energy and Technology, Geological Survey, Report 24-1, pages 31-52.

Curry, A.C., Wise, M.A. and Harmon, R.S.
2025: Trace element geochemistry of Li-rich pegmatites in the Carolina Tin-Spodumene Belt, North Carolina, USA: Implications for petrogenesis and exploration. Economic Geology, Volume 120, pages 715-743. https://doi.org/10.5382/econgeo.5144

Deer, W.A., Howie, R.A. and Zussman, J.
1992: An Introduction to the Rock-Forming Minerals, 2nd edition. Mineralogical Society of Great Britain and Ireland, 696 pages.

Dias, F., Ribeiro, R., Gonçalves, F., Lima, A., Roda-Robles, E., Martins, T. and Guimarães, D.
2025: K-Feldspar geochemistry as an indicator of lithium mineralization in the Barroso-Alvão aplite-pegmatite field, Northern Portugal. The Canadian Journal of Mineralogy and Petrology.
https://doi.org/10.3749/2500006

Dickson, W.L.
1990: Geology of the North Bay Granite Suite and metasedimentary rocks in southern Newfoundland (NTS 11P/15E, 11P/16 and 12A/2E). Government of Newfoundland and Labrador, Department of Mines and Energy, Geological Survey Branch, Report 90-3, 244 pages.

Esteves, N., Bouilhol, P., Schaltegger, U., Ovtcharova, M., Navin Paul, A. and France, L.
2025: The magmatic–hydrothermal transition record in zircon: Implications for zircon texture, composition and rare-metal granite dating (Beauvoir granite, French Massif Central). European Journal of Mineralogy, Volume 37, pages 667-693.
https://doi.org/10.5194/ejm-37-667-2025

Gale, G.H.
1966: Economic study of pegmatites, Newfoundland. Government of Newfoundland and Labrador,

Department of Mines, Agriculture and Resources, Mineral Resources Division, NFLD/0286, 33 pages.

1967: Economic assessment of pegmatites 1966. Government of Newfoundland and Labrador, Department of Mines, Agriculture and Resources, Mineral Resources Division, NFLD/0314, 117 pages.

Henry, D.J., Novák, M., Hawthorne, F.C., Ertl, A., Dutrow, B.L., Uher, P. and Pezzotta, F.
2011: Nomenclature of the tourmaline-supergroup minerals. American Mineralogist, Volume 96(5-6), pages 895-913.

Henry R.E., Groat L.A., Evans R.J., Cempírek J. and Škoda R.
2022: Crystal-chemical observations and the relation between sodium and H_2O in different beryl varieties. The Canadian Mineralogist, Volume 60, pages 625-675. https://doi.org/10.3749/canmin.2100050

Hernández-Filiberto, L., Roda-Robles, E., Simmons, W.B. and Webber, K.L.
2021: Garnet as indicator of pegmatite evolution: The case study of pegmatites from the Oxford Pegmatite field (Maine, USA). Minerals, Volume 11(8). https://doi.org/10.3390/min11080802

Hibbard, J.P., van Staal., C.R. and Miller, B.V.
2007: Links among Carolinia, Avalonia, and Ganderia in the Appalachian peri-Gondwanan realm. The Geological Society of America, Special Paper 433, pages 291-311.

Jayasinghe, N.R.
1978: Geology of the Wesleyville (2F/4) and Musgrave Harbour east (2F/5) map areas, Newfoundland. Government of Newfoundland and Labrador, Department of Mines and Energy, Mineral Development Division, Report 78-8, 15 pages.

Jochum, K.P., Weis, U., Stoll, B., Kuzmin, D., Yang, Q., Raczek, I., Jacob, D.E., Stracke, A., Birbaum, K., Frick, D.A., Günther, D. and Enzweiler, J.
2011: Determination of reference values for NIST SRM 610–617 glasses following ISO guidelines. Geostandards and Geoanalytical Research, Volume 35, pages 397-429. https://doi.org/10.1111/j.1751-908X.2011.00120.x

Knoll, T., Huet, B., Schuster, R., Mali, H., Ntaflos, T. and Hauzenberger, C.
2023: Lithium pegmatite of anatectic origin – A case study from the Austroalpine Unit Pegmatite Province (eastern European Alps): Geological data and geochemical modeling. Ore Geology Reviews, Volume 154, Article 105298. https://doi.org/10.1016/j.oregeorev.2023.105298

Koopmans, L., Martins, T., Linnen, R., Gardiner, N.J., Breasley, C.M., Palin, R.M., Groat, L.A., Silva, D. and Robb, L.J.
2024: The formation of lithium-rich pegmatites through multi-stage melting. Geology, Volume 52(1), pages 7-11.

Langille, A.E.
2012: A detailed petrographic, geochemical and geochronological study of the Hare Bay Gneiss, northeastern Newfoundland. Unpublished M.Sc. Thesis, Memorial University of Newfoundland, St. John's, Newfoundland and Labrador, 216 pages.

Lin, S., Davis, D.W., Barr, S.M., Van Staal, C.R., Chen, Y. and Constantin, M.
2007: U-Pb geochronological constraints on the evolution of the Aspy Terrane, Cape Breton Island: Implications for relationships between Aspy and Bras d'Or terranes and Ganderia in the Canadian Appalachians. American Journal of Science, Volume 307, pages 371-398.

Linnen, R.L., Van Lichtervelde, M. and Černý, P.
2012: Granitic pegmatites as sources of strategic metals. Elements, Volume 8(4), pages 275-280.

London, D.
2008: Pegmatites. Canadian Mineralogist, Special Publication 10, 347 pages.

Magyarosi, Z.
2020: Rare-element-enriched pegmatites in central Newfoundland. *In* Current Research. Government of Newfoundland and Labrador, Department of Industry, Energy and Technology, Geological Survey, Report 20-1, pages 121-143.

Malay, K.M., Archibald, D.B., Conliffe, J. and Jourdan, F.
2025: Age and mineralogy of the pollucite-bearing Hydra LCT pegmatite in southwestern Newfoundland. Oral presentation, Atlantic Geoscience Society Colloquium, Dartmouth, Nova Scotia, February 7-8, Abstracts. Atlantic Geoscience, Volume 61, page 134.

Maneta, V. and Baker, D.R.
2019: The potential of lithium in alkali feldspars, quartz, and muscovite as a geochemical indicator in the exploration for lithium-rich granitic pegmatites: A case

study from the spodumene-rich Moblan pegmatite, Quebec, Canada. Journal of Geochemical Exploration, Volume 205, Article 106336. https://doi.org/10.1016/j.gexplo.2019.106336

McCaffrey, D.M. and Jowitt, S.M.
2023: The crystallization temperature of granitic pegmatites: The important relationship between undercooling and critical metal prospectivity. Earth-Science Reviews, Volume 244, Article 104541.

Meyer, J., Tomlin, S., Green, R., Blackwood, R.F., Colman-Sadd, S.P., O'Brien, S. and Hibbard, J.
1984: Mineral occurrence map, Gander Lake, Newfoundland. Government of Newfoundland and Labrador, Department of Mines and Energy, Mineral Development Division, Map 84-045.

Müller, A., Romer, R.L. and Pedersen, R.-B.
2017: The Sveconorwegian Pegmatite Province – thousands of pegmatites without parental granites. Canadian Mineralogist, Volume 55, pages 283-315.

O'Brien, B.H., O'Brien, S.J. and Dunning, G.R.
1991: Silurian cover, Late Precambrian–Early Ordovician basement, and the chronology of Silurian orogenesis in the Hermitage Flexure (Newfoundland Appalachians). American Journal of Science, Volume 291(8), pages 760-799.

O'Brien, S.
1982: Peter Snout, east half, Newfoundland. Map 82-058. Government of Newfoundland and Labrador, Department of Mines and Energy, Mineral Development Division, Open File 11P/13/0097.

O'Brien, S.J., Knight, I. and Blackwood, R.F.
1987: St Brendans, Bonavista North District, Newfoundland. Map 87-055. Government of Newfoundland and Labrador, Department of Mines, Mineral Development Division, Open File 2C/13/0055.

O'Neill, P.P.
1990: Geology of the northeast Gander Lake map area (NTS 2D/15) and the northwest Gambo map area (NTS 2D/16). *In* Current Research. Government of Newfoundland and Labrador, Department of Mines and Energy, Geological Survey Branch, Report, 90-1, pages 317-326.

1991: Geology of the Weirs Pond area, Newfoundland (NTS 2E/1). Government of Newfoundland and Labrador, Department of Mines and Energy, Geological Survey Branch, Report 91-3, 164 pages.

1992: Geology of the northwestern part of the Glovertown map area (NTS 2D/9) and the northeastern part of the Dead Wolf Pond map area (NTS 2D/10). *In* Current Research. Government of Newfoundland and Labrador, Department of Mines and Energy, Geological Survey Branch, Report 92-1, pages 195-202.

Paton, C., Hellstrom, J., Paul, B., Woodhead, J. and Hergt, J.
2011: Iolite: Freeware for the visualisation and processing of mass spectrometric data. Journal of Analytical Atomic Spectrometry, Volume 26, pages 2508-2518. https://doi.org/10.1039/C1JA10172B

Pearce, N.J.G., Perkins, W.T., Westgate, J.A., Gorton, M.P., Jackson, S.E., Neal, C.R. and Chenery, S.P.
1997: A compilation of new and published major and trace element data for NIST SRM 610 and NIST SRM 612 glass reference materials. Geostandards Newsletter, Volume 21, pages 115-144. https://doi.org/10.1111/j.1751-908X.1997.tb00538.x

Pollock, J.C., Hibbard, J.P. and van Staal, C.R.
2012: A paleogeographical review of the peri-Gondwanan realm of the Appalachian orogen. Canadian Journal of Earth Science, Volume 49, pages 259-288.

Roda-Robles, E., Vieira, R., Lima, A., Errandonea-Martin, J., Pesquera, A., Cardoso-Fernandes, J. and Garate-Olave, I.
2023: Li-rich pegmatites and related peraluminous granites of the Fregeneda-Almendra field (Spain-Portugal): A case study of magmatic signature for Li enrichment. Lithos, Volume 452-453, Article 107195. https://doi.org/10.1016/j.lithos.2023.107195

Saha, D., Archibald, D.B., Conliffe, J. and Jourdan, F.
2025: Lithium-cesium-tantalum (LCT) pegmatites in southern Newfoundland. Oral presentation, Atlantic Geoscience Society Colloquium, Dartmouth, Nova Scotia, February 7-8, Abstracts. Atlantic Geoscience, Volume 61, pages 148-149.

Schulz, K.J., Stewart, D.B., Tucker, R.D., Pollock, J.C. and Ayuso, R.A.
2008: The Ellsworth terrane, coastal Maine: Geochronology, geochemistry, and Nd-Pb isotopic composition–Implications for the rifting of Ganderia. Geological Society of America Bulletin, Volume 120, pages 1134-1158.

Sun, S.S. and McDonough, W.F.
1989: Chemical and isotopic systematics of oceanic basalts: implications for mantle composition and processes. Geological Society, London, Special Publications, Volume 42(1), pages 313-345.

Tater, J.M.
1964: A field report on pegmatitic occurrences of Newfoundland. Newfoundland and Labrador Geological Survey, Internal Collection, University Report, 55 pages, [Geofiles # NFLD/0258].

Tischendorf, G., Rieder, M., Förster, H.J., Gottesmann, B. and Guidotti, C.V.
2024: A new graphical presentation and subdivision of potassium micas. Mineralogical Magazine, Volume 68(4), pages 649-667.

Tvauri, A.V., Kalliomäki, H., Rämö, O.T., Law, K.A., Ranta, E. and Beier, C.
2025: Tourmaline and muscovite chemistry as a proxy for the origin and evolution of Paleoproterozoic lithium pegmatites in Kaustinen, western Finland. Lithos, Volume 518-519, Article 108306.
https://doi.org/10.1016/j.lithos.2025.108306

USGS (U.S. Geological Survey)
2025: Mineral commodity summaries 2025 (ver. 1.2, March 2025): U.S. Geological Survey, 212 pages.
https://doi.org/10.3133/mcs2025

Valverde-Vaquero, P., van Staal, C.R., McNicoll, V. and Dunning, G.R.
2006: Mid–Late Ordovician magmatism and metamorphism along the Gander margin in central Newfoundland. Journal of the Geological Society, Volume 163, pages 347-362.
https://doi.org/10.1144/0016-764904-130

van Lichtervelde, M., Laurent, O., Amponsah, P.O. and Williams, I.I.E.
2025: Dating multiple fractionation trends in pegmatites – Implications for the genesis of a large lithium pegmatite province in West-Africa. Chemical Geology, Volume 691, Article 122935.
https://doi.org/10.1016/j.chemgeo.2025.122935

van Staal, C.R. and Barr, S.M.
2012: Lithospheric architecture and tectonic evolution of the Canadian Appalachians and associated Atlantic margin. *In* Tectonic Styles in Canada: The LITHOPROBE Perspective. *Edited by* J.A. Percival, F.A. Cook and R.M. Clowes. Geological Association of Canada, Special Paper 49, pages 41-95.

van Staal, C.R., Barr, S.M. and Murphy, J.B.
2012: Provenance and tectonic evolution of Ganderia: Constraints on the evolution of the Iapetus and Rheic oceans. Geology, Volume 40(11), pages 987-990.

van Staal, C.R., Barr, S.M., Waldron, J.W.F., Schofield, D.I., Zagorevski, A. and White, C.E.
2021: Provenance and Paleozoic tectonic evolution of Ganderia and its relationships with Avalonia and Megumia in the Appalachian-Caledonide orogen. Gondwana Research, Volume 98, pages 212-243.

van Staal, C.R., Sullivan, R.W. and Whalen, I.
1996: Provenance and tectonic history of the Gander margin in the Caledonian/Appalachian orogen: Implication for the origin and assembly of Avalonia. *In* Avalonian and Related Peri-Gondwanan Terranes of the Circum-North Atlantic: Boulder, Colorado. *Edited by* D. Nance and M. Thompson. Geological Society of America, Special Paper 304, pages 347-367.

Wang, C., Wang, T., van Staal, C.R., Hou, Z. and Lin, S.
2024: Evolution of Silurian to Devonian magmatism associated with the Acadian orogenic cycle in eastern and southern Newfoundland Appalachians: Evidence for a three-stage evolution characterized by episodic hinterland-and foreland-directed migration of granitoid magmatism. Geological Society of America Bulletin, Volume 136(11-12), pages 4648-4670.

Whitney, D.L. and Evans, B.W.
2010: Abbreviations for names of rock-forming minerals. American Mineralogist, Volume 95, pages 185-187.

Williams, H.
1979: Appalachian Orogen in Canada: Canadian Journal of Earth Sciences, Volume 16, pages 792-807.
https://doi.org/10.1139/e79-070

Wise, M.A., Curry, A.C. and Harmon, R.S.
2024: Reevaluation of the K/Rb-Li systematics in muscovite as a potential exploration tool for identifying Li mineralization in granitic pegmatites. Minerals, Volume 14, Article 117. https://doi.org/10.3390/min14010117